

Article

Cleaner Approach for Atrazine Removal Using Recycling Biowaste/Waste in Permeable Barriers

Ana Lago *, Bruna Silva and Teresa Tavares 

Centre of Biological Engineering, Campus de gualtar, University of Minho, 4710-057 Braga, Portugal; bsilva@ceb.uminho.pt (B.S.); ttavares@deb.uminho.pt (T.T.)

* Correspondence: analago@ceb.uminho.pt; Tel.: +351-253-601976; Fax: +351-253-604429

Abstract: This work addresses the rehabilitation of water contaminated with atrazine, entrapping it in a permeable and sustainable barrier designed with waste materials (sepiolite) and with biomaterials (cork and pine bark). Atrazine adsorption was assessed by kinetics and equilibrium assays and desorption was tested with different extraction solvents. Adsorbed atrazine was 100% recovered from sepiolite using 20% acetonitrile solution, while 40% acetonitrile was needed to leach it from cork (98%) and pine bark (94%). Continuous fixed-bed experiments using those sorbents as PRB were performed to evaluate atrazine removal for up-scale applications. The modified dose-response model properly described the breakthrough data. The highest adsorption capacity was achieved by sepiolite (23.3 (± 0.8) mg/g), followed by pine bark (14.8 (± 0.6) mg/g) and cork (13.0 (± 0.9) mg/g). Recyclability of sorbents was evaluated by adsorption-desorption cycles. After two regenerations, sepiolite achieved 81% of atrazine removal, followed by pine with 78% and cork with 54%. Sepiolite had the best performance in terms of adsorption capacity/stability. SEM and FTIR analyses confirmed no significant differences in material morphology and structure. This study demonstrates that recycling waste/biowaste is a sustainable option for wastewater treatment, with waste valorization and environmental protection.

Keywords: emerging pollutants; waste-based adsorbents/biosorbents; eco-friendly process; permeable barriers; reusability; circular economy



Citation: Lago, A.; Silva, B.; Tavares, T. Cleaner Approach for Atrazine Removal Using Recycling Biowaste/Waste in Permeable Barriers. *Recycling* **2021**, *6*, 41. <https://doi.org/10.3390/recycling6020041>

Academic Editors: Ismael Leonardo Vera Puerto and Carlos A. Arias

Received: 14 May 2021
Accepted: 11 June 2021
Published: 17 June 2021

Publisher's Note: MDPI stays neutral with regard to jurisdictional claims in published maps and institutional affiliations.



Copyright: © 2021 by the authors. Licensee MDPI, Basel, Switzerland. This article is an open access article distributed under the terms and conditions of the Creative Commons Attribution (CC BY) license (<https://creativecommons.org/licenses/by/4.0/>).

1. Introduction

Herbicides are a type of pesticides used to specifically target weeds and other unwanted plants. They are considered emerging contaminants that have become a threat to water supply network. Although they are found in effluents of wastewater treatment plants (WWTP) and in surface water at trace levels (normally ranging from ng/L to $\mu\text{g/L}$) [1], their fate, behavior and persistence in the environment became a threat to aquatic and terrestrial biodiversity and human health [2].

Atrazine (2-chloro-4-ethylamino-6-isopropylamino-1,3,5-triazine) is a recalcitrant compound and an organonitrogen herbicide extensively used to control broadleaf and grass weeds [3]. This herbicide does not tend to bioaccumulate, but its permanence in the environment and mobility in some soils can lead to surface and groundwater contamination [4]. In fact, atrazine is commonly found in drinking water at levels exceeding 0.1 $\mu\text{g/L}$ [3–6] as a result of its massive use in agriculture. It is registered in more than 70 countries, making it the most commonly detected pesticide in surface water in the United States and also frequently detected in groundwater as well [7]. Its use has been banned among the European countries since 2003, due its potential threat to human health, its endocrine-disrupting nature and embryotoxic and embryo-lethal functions [3,4].

The Directive 2013/39 EU [8] states that atrazine is an environmental contaminant and a xenobiotic, considered one of the priority substances in the field of water policy justifying the urgency to develop cheaper and more effective water treatments to reduce its impact on the environment. The presence of herbicides in aquatic matrices is mainly

attributed to the discharge of municipal effluents with inefficient treatment by WWTP [2,9]. Some alternatives can be applied to remove these molecules from wastewater. Adsorption with commercial activated carbon (AC) is one of the most preferential techniques for water reuse [10], due to its very high specific surface area, microporosity, adsorptive capacities and insensitivity to toxic pollutants [11]. However, the use of commercialized AC also presents disadvantages such as a high cost of production and non-renewable source origin, high regeneration costs [12] and high demand [13]. Therefore, cheap, renewable and sustainable alternative adsorbent materials should be tested, optimized and implemented for water and wastewater treatment.

Recently, technologies that use adsorbents produced from biomass have attracted much attention from researchers since they are biodegradable, and they have a good mechanical and chemical resistance, as they are widely available in nature. The usage of biosorbents defines a low-cost technology and viable approach to remove herbicides from water due to their physical and chemical affinity [14]. Additionally, waste-based materials, whether organic or inorganic, are seen as promising adsorbents for water and wastewater treatment due to their local availability, cost-effectiveness, technical feasibility and applicability [15]. By recycling waste, its life cycle is increased and circular economy is promoted. Studies on the use of waste (biosorbents or adsorbents) to remove pollutants are gaining more significance within the research community, as revealed by the growing number of published works [12,15–17].

Different waste-based materials can be used for herbicide removal, such as sand, sediment and soil, clays, dairy manure, agricultural and industrial waste, AC derived from biomasses and waste, and rubber granules, among others [3,18–21]. Clay minerals have been widely applied to adsorb different molecules due to their availability, large specific surface area, low cost, chemical and mechanical stability [22–25]. Among clays, the relevant chemical properties of sepiolite, a naturally occurring hydrated magnesium silicate of sedimentary origin, have encouraged several authors to assess its efficiency on the adsorption of different organic and inorganic pollutants [26–28]. Its structure is responsible for its relevant specific surface area and high porosity, providing substantial surface sites for adsorption processes [29]. Sepiolite is widespread and abundant on earth, and can be purchased at a low cost. It can also be classified as an inorganic waste from its exploitation deposits or from its processing and purification processes [30]. Bark from *Pinus pinaster* generated by the forestry industry is one of the most abundant sources of agro-forestry lignocellulosic waste in Europe. Due to its high production volume and biodegradability, new technologies for its reutilization are currently being produced. Pine bark has been proposed as biosorbent to remove different pollutants from contaminated water and wastewater due to its high potential sorption capacity by ion exchange and chelating processes [15,31]. Furthermore, cork, the outer bark of the oak tree (*Quercus suber*), has been valued as a natural adsorption substrate for the removal of a broad range of pollutants [14,31,32]. Cork has interesting properties such as low density, buoyancy and important binding sites present on its structure [32]. Due to its unique characteristics, its availability in cork-producing areas or the low cost acquisition of used cork stoppers and cork powder rejected by industry, the use of cork as an adsorbent has become an interesting alternative in the field of wastewater treatment [15]. Often, spent tires are dumped in open or landfill sites; however, because of their abundance and low cost they could be recycled and turned into a viable alternative adsorbent [33]. The structural characteristics of sorbents can be changed by physical and chemical treatments, and their adsorption capacity improved. Pyrolysis processes allow an increase in the specific surface area of the waste rubber, and the use of an activation agent favors the porosity of AC [34]. Activated chars produced from tire rubber waste have been studied by the research community, to adsorb different compounds from wastewater [34,35].

The concept of permeable reactive barriers (PRB) emerged as a most promising and widely accepted technology for the remediation of contaminated groundwater [28]. PRB entails the emplacement of an engineered highly permeable reactive material in the sub-

surface, filled perpendicular to groundwater flow direction, to treat contaminated plumes in situ transported by the natural groundwater flow [36,37]. During the residence of the polluted groundwater in the barrier, target contaminants are immobilized, adsorbed and/or transformed into less toxic and harmful forms due to different physical, and/or bio-chemical processes occurring in the solid support [38]. The reactive constituent is selected based on the retention capacity of the material towards the target hazardous molecule(s) [39], its life time and its sensibility to the influence of external constituents. PRB optimization is usually performed in batch experiments and in continuous column assays, under the same environmental conditions to reproduce groundwater flow [38].

In addition to the low cost and the availability waste materials, the economic feasibility of an adsorption process will also depend on the adsorption capacity of the material and recyclability over time. It is important to consider the desorption of contaminants and the regeneration capability in the selection of an adequate adsorbent. Regeneration over adsorbent replacement can significantly improve the lifetime of PRB. The use of solvents to chemically regenerate adsorbents and recover adsorption capacity becomes feasible and attractive. The main advantages of this process are the possibility to extract/recover target substances and the low mass loss of the adsorbent [40]. There are several reported waste-based materials with proven sorption capacity; however, very few studies report their proneness to regeneration [41]. Some of the reported materials are not easily regenerated, as their morphology and adsorption capacity are affected after desorption processes [31]. The selection of an effective, but also eco-friendly and competitive, desorption process that enables adsorbent reusability is a crucial step of the overall project.

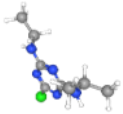
Previous studies have reported the adsorption characteristics of atrazine onto some reusable biomaterials/materials without pre-treatments in laboratory experiments [3,14,42,43], but the novelty of this study is the assessment of the capacity of sepiolite, cork and pine bark particles without previous resort to chemicals, to function as reactive constituents of PRB to remediate atrazine-contaminated aquifers. It was possible to produce data from batch experiments on adsorption behavior and capacities, rates and regeneration proneness for the tested materials, crucial to evaluate the performance of PRB columns to remediate atrazine contaminated plumes. Moreover, the recovery effectiveness and recyclability of the selected biomaterials by an optimized desorption process was demonstrated. Adsorption of atrazine on activated waste rubber char was also performed in batch mode for comparison with other materials without pretreatment. The present research is in line with the growing concern and demand for information on herbicide removal with the use of sustainable waste-based biomaterials/materials with their recovery after usage and proven recycling ability, expected by environmental policies.

2. Materials and Methods

2.1. Chemicals

Atrazine (PESTANAL[®] analytical standard, 99.1%) was purchased from Sigma-Aldrich (St. Louis, MO, USA). Table 1 summarizes the major physicochemical properties of atrazine. To increase water solubility, atrazine was dissolved in acetonitrile (HPLC grade) and a stock solution of 1g/L was stored. Diluted solutions of atrazine were prepared from the stock solution using deionized water. For the determination of pH of zero point of charge (pH_{zpc}), 1.0 M H_2SO_4 (95%, Fisher Chemical, Leicestershire, UK), 1.0 M NaOH ($\geq 97\%$, Fisher Chemical) and 0.01 M NaCl (99.5%, PanReac, Barcelona, Spain) solutions were prepared. hPLC-grade acetonitrile (Fisher Chemical) and ultra-pure water, obtained from a Milli-Q Millipore system (Merck, Darmstadt, Germany), were used to prepare the mobile phases for atrazine quantification using ultra-high performance liquid chromatography with diode array detector (UHPLC-DAD, Shimadzu Corporation, Kyoto, Japan). Acetate buffer was prepared by diluting sodium acetate ($\geq 99\%$ Fisher Chemical) and acetic acid ($\geq 99.7\%$, Fisher Chemical) in water, and potassium phosphate buffer was prepared by diluting di-potassium hydrogen orthophosphate ($\geq 99\%$, Fisher Chemical) and potassium di-hydrogen phosphate (99%, PanReac) in water.

Table 1. Selected physicochemical properties of atrazine.

Chemical Name	Molecular Formula	Structure (3D) [44]	Molecular Weight (g/mol)	Water Solubility (mg/L at 25 °C) [44]	pKa [45]	Log K _{ow} [45]	Molar Volume (cm ³ /mol)	Width (Å) [46]	Depth (Å) [46]	Thickness (Å) [46]
Atrazine	C ₈ H ₁₄ ClN ₅		215.69	33	1.68	2.6–2.71	169.8	9.6	8.4	~3

2.2. Preparation of Waste-Based Adsorbents/Biosorbents

Natural sepiolite was supplied by Tolsa S.A. located in Madrid, Spain. Firstly, the clay mineral was sieved to obtain a particle size with equivalent diameter between 1 and 2 mm and then it was washed with deionized water to remove dust. It was placed in an oven at 60 °C for 24 h and stored in a desiccator for further use.

Cork stoppers were supplied by a cork producing industry, Corticeira Amorim, SGPS, S.A. located in Aveiro, Portugal. The stoppers received were cut into small pieces and milled. The grains were sieved to a size with equivalent diameter between 1 and 2 mm and then washed with deionized water to remove dirt and particulate materials. The cleaned cork was placed in an oven at 60 °C for 24 h and then stored in a desiccator.

Pine bark was collected from a pine forest located in Braga, Portugal. It was washed with deionized water to remove mud, other materials and impurities and then placed in an oven at 60 °C to be dried. Then, it was ground into smaller particles, sieved in the range of 1 mm to 2 mm and stored in a desiccator.

Activated rubber char material was prepared using the pyrolysis of waste rubber granules provided from a truck tires and rubber waste recycling company, Eco-recycling LTD, located in Novi Sad, Serbia. Pyrolysis and activation processes were performed at the Department of Materials, Vinča Institute of Nuclear Sciences, Belgrade, Serbia. The waste rubber granules were pyrolyzed into a quartz tube furnace under an N₂ flow at 800 °C for 4 h (heating rate was 5 °C/min). After this procedure, the char was washed with 2 M hNO₃ to clean the sample surface from metals. Carbonized granules and the solution of 2 M hNO₃ were mixed on a magnetic stirrer for 2 h at room temperature, filtered, washed with distilled water and dried in an oven at 110 °C. After that, the material was mixed with KOH pellets (sample/KOH = 1/4) and activated at 800 °C for 4 h under N₂ atmosphere. In order to remove the impurities, the resulting activated carbon-based powder was washed with 0.5 M hCl solution (mixed in a magnetic stirrer at 85 °C for 30 min). Lastly, the sample was washed with deionized water and dried in an oven at 110 °C.

2.3. Materials Characterization

The pH_{zpc} of materials was determined, as it helps to explain the electrostatic interactions between adsorbate and sorbent. A solution of 0.01 M NaCl was prepared, previously bubbled with nitrogen to avoid the dissolution of atmospheric CO₂ and to prevent a change in the solution's pH. Solutions with pH values from 1 to 9 were prepared by adding 1.0 M H₂SO₄ or 1.0 M NaOH. For each pH value, 0.1 g of adsorbent was added to 25 mL of NaCl solution in 50 mL falcons. Flasks were sealed to avoid contact with air and were kept under moderate agitation in an incubator at 25 °C for 48 h. Afterwards, the adsorbent was filtered and the pH of the remaining solution was measured and plotted against the initial pH. The pH_{zpc} is defined as the pH at which the curve crosses the line pH_{initial} = pH_{final}.

The surface morphology of adsorbents (before atrazine adsorption and after adsorption-desorption cycles) was examined by Scanning electron microscopy (SEM) by a Phenom ProX scanning electron microscope (Phenom-World BV, Eindhoven, The Netherlands). All data were processed using the ProSuite software (Thermo Fisher, Boston, MA, USA). The observation of samples was performed with gold coating.

The presence of functional groups in the surfaces (in their natural form and after the first and the second desorption steps) was evaluated by attenuated total reflection Fourier-

transform infrared (ATR-FTIR) spectroscopy using an ALPHA II- Bruker spectrometer (Ettlingen, Germany) with a diamond-composite cell. The measurements were recorded over the range from 4000 to 400 cm^{-1} , with a resolution of 4 cm^{-1} and 24 scans per sample.

2.4. Quantification of Atrazine

Atrazine quantification was performed by UHPLC-DAD, using a Shimadzu Nexera X2 and a Kinetex C18 column (Phenomenex, Torrance, CA, USA) (1.7 $\mu\text{m} \times 100 \text{ \AA} \times 2.1 \text{ mm}$), operating in gradient mode. Eluents used were acetonitrile and ultrapure water (45:55 *v/v* %) at a flow rate of 0.2 mL/min. The autosampler and column temperature was kept at 25 °C, and an injection volume of 5 μL was used. The chromatograms were registered at atrazine maximum adsorption wavelength at 225 nm. The linearity of the method was assured by setting a calibration curve over the concentration range of 0.3–4 mg/L. Detection limit (0.1 mg/L) was determined as the minimum detectable concentration of the analyte in the test sample that can be reliably distinguished from zero. The quantification limit (0.3 mg/L) was set as the concentration above which the analytical method operates with precision. The average peak area of each standard was used for quantification. Data were processed by Lab Solutions software (version 5.71, Shimadzu Corporation, Kyoto, Japan).

2.5. Batch Experiments

Kinetics and equilibria experiments were performed to evaluate the atrazine adsorption capacity of different adsorbents/biosorbents. A predetermined mass of each material was placed in amber Erlenmeyer flasks, and a fixed volume of the atrazine stock solution with 2 mg/L was added. Desorption experiments were carried out to evaluate the desorption capacity of atrazine from sepiolite, cork and pine bark using different extraction solvents. To assure the reproducibility of the results, each assay was performed in triplicate and the average of the three assays was reported for each test. The experiments were conducted in the absence of light to avoid the photo degradation of the herbicide [47].

Experiments with activated rubber char were performed as a comparative term. Due to the high material production costs, reduced availability and different particle size, only batch kinetics and equilibria tests were performed with this material.

2.5.1. Adsorption Kinetics

Assays were performed to determine the equilibrium adsorption time and to evaluate the adsorption rate of atrazine onto the sorbents. Adsorbent doses of 1 g/L of activated rubber char, and 5 g/L for sepiolite, cork and pine bark were used for equilibria assessment. Each mass of adsorbent was placed in contact with 50 mL of 2 mg/L of atrazine solution in Erlenmeyer flasks and these were shaken in a temperature-controlled incubator at 140 rpm and 25 °C until equilibrium was reached (14 h for the activated rubber char, 56 h for sepiolite, 72 h for cork and 8 days for pine bark). For the kinetics, samples were taken at different time intervals from another set of erlenmeyers, filtered through 0.22 μm nylon syringe filters, and the filtrate was analyzed for atrazine concentration by UHPLC-DAD. A blank test, with 2 mg/L of atrazine without biosorbent/adsorbent material, was performed in an Erlenmeyer flask and analyzed during the experiment. To determine the adsorption capacity, q_t (mg/g), the following Equation (1) was used:

$$q_t = \frac{(C_0 - C_t) V}{m} \quad (1)$$

where C_0 (mg/L) is the initial concentration of atrazine in solution, C_t (mg/L) is the remaining concentration of atrazine in solution at time t , V (L) is the initial volume of the solution, and m (g) is the mass of the adsorbent material.

The experimental data were fitted by Lagergren pseudo-first order (PFO) [48] (Equation (2)) and pseudo-second order (PSO) [49] (Equation (3)) models to describe atrazine

adsorption kinetics. Origin Pro 8.0 software (OriginLab, Northampton, MA, USA) was used to perform the calculations.

$$q_t = q_e [1 + \exp(-k_1 \cdot t)] \quad (2)$$

$$q_t = \frac{k_2 \cdot q_e \cdot t}{1 + k_2 \cdot q_e \cdot t} \quad (3)$$

q_t is the adsorption capacity at time t (mg/g), q_e is the adsorption capacity at equilibrium time (mg/g), and k_1 (min^{-1}) and k_2 (g/mg.min) are the adsorption rate constants of PFO and PSO, respectively.

2.5.2. Adsorption Equilibrium

Once the equilibrium time for each sorbent was established, equilibrium experiments were performed to build up the adsorption isotherms and to determine the maximum uptake value for each material. Activated rubber char concentrations tested ranged between 0.05 and 0.75 g/L, while for sepiolite, cork and pine bark they ranged from 1 to 15 g/L. Different amounts of each adsorbent were placed in contact with 2 mg/L of atrazine solution in amber Erlenmeyer flasks. The flasks were kept under continuous stirring at 140 rpm and 25 °C, during the period of time needed to attain the equilibrium. Samples were then taken, filtered and analyzed by UHPLC to determine the remaining atrazine concentration. The adsorption capacity of sorbents at equilibrium q_e (mg/g) was determined using Equation (1), where C_0 is substituted by C_e (mg/L), equilibrium concentration of atrazine in solution.

Freundlich [50] and Sips [51] isotherm models (Equations (4) and (5), respectively) were applied to equilibrium results to evaluate adsorption behavior:

$$q_e = K_F \cdot C_e^{\frac{1}{n}} \quad (4)$$

K_F represents the relative adsorption capacity [(mg/g)(L/mg) $^{1/n}$] and n is a constant (dimensionless) related with the degree of non-linearity of the Equation.

$$q_e = \frac{q_{max} \cdot K_s \cdot C_e^{\frac{1}{m_s}}}{1 + K_s \cdot C_e^{\frac{1}{m_s}}} \quad (5)$$

K_s is the affinity constant related to the adsorption energy (L/g) and m_s is a parameter related with the heterogeneity of the system.

2.5.3. Desorption Behavior

Batch assays were performed using 0.75 g of sorbents in 50 mL of 2 mg/L atrazine solution (solid/liquid ratio of 15 g/L) at 25 °C, during the time needed to reach equilibrium for each material (56 h for sepiolite, 72 h for cork and 8 days for pine bark). Then, samples were taken, filtered and analyzed by UHPLC to quantify the atrazine remaining in solution. The suspensions were filtered, the materials were recovered and dried at 30 °C. Atrazine desorption assessment was then conducted by using the following extraction solvents: acetate buffer at pH 5, potassium phosphate buffer at pH 7, aqueous solutions with 5%, 20% and 40% (except for sepiolite) acetonitrile at 25 °C and deionized water at 25 °C, 40 °C and 60 °C. In detail, sorbents loaded with atrazine were mixed with 50 mL of each extraction solvent (using 15 g/L of sorbent concentration) under continuous agitation at 140 rpm for 24 h. Liquid samples were collected at regular intervals and filtered, and the efficiency of atrazine desorption was evaluated through UHPLC analysis as described previously. The desorption percentage, D (%) was calculated by using Equation (6):

$$D(\%) = \frac{C_{des}}{C_{ads}} \times 100 \quad (6)$$

Here, C_{des} is the concentration of desorbed atrazine along the time and C_{ads} the initial concentration of adsorbed atrazine on adsorbent.

2.6. Column Adsorption Experiments

Column adsorption using a PRB at lab scale in continuous flow to treat 2 mg/L aqueous solution of atrazine allowed to determine operational parameters as breakthrough and exhaustion time, useful for process design and upscale. Regeneration and reusability assays and PRB simulation with sepiolite, cork and pine bark as supports were performed in column systems at lab scale. Consecutive adsorption of atrazine from 2 mg/L solution and desorption processes (using the extraction solvent with the best desorption capacity obtained for each material) were carried out to establish the adsorption capacity profile of each material after several adsorption-desorption cycles. To assure the reproducibility of the results, each assay was performed in duplicate and the average of both assays is reported for each test. The experiments were conducted in the absence of light to avoid the photo-degradation of the herbicide.

2.6.1. Regeneration and Reusability

The viability of adsorbents depends on their effective reuse, so the evaluation of adsorbent recyclability becomes necessary. The operation of a column with a fixed barrier for cyclic adsorption/desorption processes is an effective technique for the purpose, as it makes the best use of the concentration difference driving force for adsorption and a more efficient utilization of the adsorbent capacity. The repetitive adsorption-desorption cycles were performed to determine the loss in the uptake capacity of the adsorbents. 20 g of each material was placed inside an acrylic column (height: 30 cm, internal \varnothing 4 cm) and a predetermined volume of 2 mg/L atrazine solution (using a solid/liquid ratio 15 g/L) was added. The pollutant influent was introduced into the column from the bottom to the top in closed-loop mode at a controlled flow rate of 1 mL/min for 96 h, 72 h and 83 h for sepiolite, cork and pine bark, respectively. When equilibria were reached, column operation stopped and the excess atrazine solution inside the columns was withdrawn. The regeneration of the adsorbent by desorption processes initiated in continuous mode over 48 h with the selected extraction solvents, aqueous solution with 20% acetonitrile for sepiolite and 40% acetonitrile solution for cork and pine bark. Materials were regenerated twice and reused another 2 times. During adsorption and desorption cycles, samples were collected periodically from the outflow of the column to determine atrazine concentration by UHPLC. To assure the reproducibility of the results, each assay was performed in duplicate and the average of two assays was reported for each test.

2.6.2. PRB Simulation at Lab Scale

The use of PRB in a continuous flow column is a practical and efficient technique to remove pollutants from real wastewater. The ability of the waste-based sepiolite, cork and pine bark to function as effective PRB for the removal of atrazine at 2 mg/L was evaluated in open system experiments (continuous flow) at a laboratory scale. The continuous column experiments were operated using three individual acrylic columns (height: 30 cm, internal \varnothing 4 cm), each one filled with 20 g of each material. Atrazine solution was fluxed upwards through the columns using a peristaltic pump at 1 mL/min for 76 h without recirculation. Periodically, samples were collected in the outflow to determine atrazine concentration by UHPLC until exhaustion time was reached. The assays were conducted in duplicate and the results are an average of the duplicates. Breakthrough curves were obtained by plotting the normalized concentration values (C_t/C_0) versus time.

Adsorption dynamics acquaintance and modelling are essential because they provide valuable information on some practical aspects such as sorbent capacity and prediction of the time necessary for the effective operation of a PRB column. Among the different mathematical models that can be used to describe the removal behavior of a certain pollutant, the modified dose-response [52] (Equation (7)) and Yoon-Nelson [53] (Equation (8)) models

were selected to predict breakthrough curves and to determine the characteristic parameters of the column that are useful for process design, with nonlinear regression fitting. In this model, α is the parameter that is associated with the shape of the breakthrough curve. When $\alpha \leq 1$, the model displays a parabola-like curve, and for $\alpha > 1$ the curve assumes a sigmoidal shape [28].

$$\frac{C}{C_0} = 1 - \frac{1}{1 + \left(\frac{C_0 \cdot Q \cdot t}{q_0 \cdot m_B}\right)^\alpha} \quad (7)$$

Q is the flow rate (mL/min), q_0 is the adsorption capacity of the bed (mg/g), m_B is the mass of the adsorbent (g) and α is a dimensionless empirical constant.

$$\frac{C}{C_0} = \frac{1}{1 + \exp(k_{YN} \cdot \tau - k_{YN} \cdot t)} \quad (8)$$

k_{YN} (h^{-1}) is the Yoon-Nelson rate coefficient, τ (h) is the time required to retain 50% of the initial adsorbate and t is the operating time (min).

2.7. Statistical Analysis

GraphPad Prism[®] software (version 8.0; graphPad Software, Inc., San Diego, CA, USA) was used for statistical analyses. The level of significance was determined by two-ways ANOVA followed by Tukey's test for multiple comparisons. Significance was accepted at $p < 0.05$.

3. Results and Discussion

3.1. Characterization of the Adsorbents/Biosorbents

The pH_{zpc} is of fundamental importance in surface science applied to environmental rehabilitation, since it allows to determine the ability of a substrate to retain the molecules of interest. This parameter is relevant in adsorption processes since it influences the solution pH and the electrostatic interactions between adsorbate and adsorbent. This parameter is described as the pH at which the net charge of the adsorbent surface is equal to zero. At a pH lower than pH_{zpc} , the surface of the adsorbent is positively charged, favoring anions species to be adsorbed. On the opposite, when the pH is higher than pH_{zpc} , the surface of the adsorbent is negatively charged and cations will be preferentially adsorbed. In Figure 1, the results obtained for pH_{zpc} determination by the pH drift method are shown. The pH_{zpc} is identified as the point where the line $\text{pH}_{\text{initial}} = \text{pH}_{\text{final}}$ crosses the experimental pH curve. Sepiolite presents a pH_{zpc} value around eight, while for cork and pine bark the obtained pH_{zpc} values are three and five, respectively.

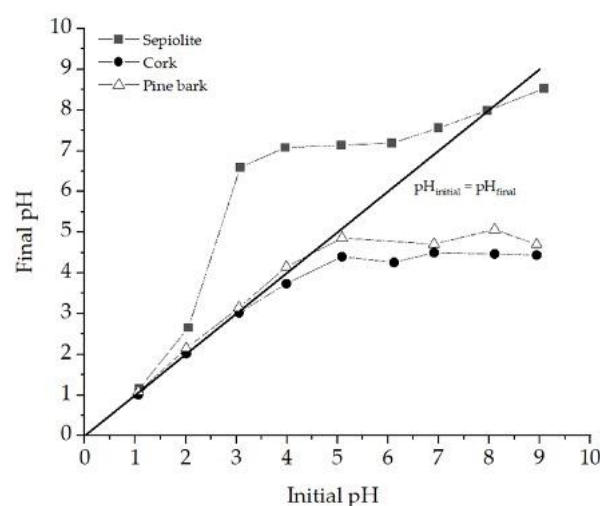


Figure 1. Determination of pH_{zpc} of sepiolite, cork and pine bark using the pH drift method.

Atrazine is considered a very weak base, with a pK_a value of 1.68 and an isoelectric point (pI) of 9.23. Under the conditions of the study, the pH of atrazine solution at 2 mg/L has a value of 5.7. When atrazine molecules are in contact with the sorbent materials, their pH changes because of the ionic interactions between adsorbate and adsorbent.

Figure 2 shows the charge distribution of atrazine at different pH levels. Increasing pH led to progressive deprotonation of the functional groups from the surface. Atrazine molecules are in the neutral form in the range of pH between 6.5 and 11.5. Atrazine is positively charged for pH values lower than 6.5, and negatively charged at pH higher than 11.5.

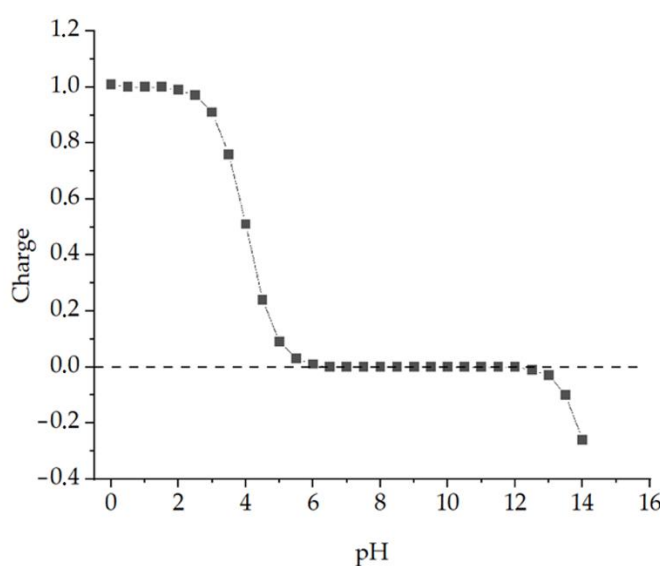


Figure 2. Charge distribution of atrazine as a function of pH (plot obtained using Marvin Sketch tool).

According to pH_{zpc} study, cork and sepiolite surfaces assume a negative charge when in contact with atrazine solution, once the solution pH is higher than their pH_{zpc} . On the other hand, pine bark surface becomes neutral, once solution pH is at the same pH_{zpc} value. By ion-exchange mechanism, the atrazine molecule is favorably adsorbed by cork. Table 2 summarizes the charge distribution interactions of sorbent materials, when in contact with atrazine solution.

Table 2. Charges distribution of atrazine molecule and sorbents surface through solution pH.

Waste Material	pH Variation	Atrazine Molecule Charge	Sorbents Surface Charge
Cork	5.7–5.39	+	-
Pine bark	5.7–4.62	+	neutral
Sepiolite	5.7–9.2	neutral	-

SEM has been used as a primary tool to characterize the surface morphology and the essential physical properties of the adsorbents, such as porosity and structure. Sepiolite, pine and cork (before adsorption experiments and after two regeneration cycles), as well as activated rubber char samples were analyzed by SEM (Figure 3). Raw sepiolite (Figure 3A) exhibits a micro-fibrous texture, with inter-fibers/bundles spaces. Its textural properties were reported in previous works by this research group: surface area (S_{BET}) of 181.35 m²/g, pore volume of 0.30 cm³/g and average pore size of 65.8 Å [28]. Figure 3C shows a radial view of a ray of *Pinus pinaster* bark constituted of small pits. *Quercus suber* (Figure 3E) shows a porous surface formed from adjacent hollow polyhedral prismatic cells, similar to a honeycomb structure. Cork and pine bark present a very low specific surface area (<4 m²/g [15]). Figure 3G exhibits a particle of rubber char (dark area) activated with KOH (white area). This activated char is essentially mesoporous, with a high S_{BET} value

and pore volume. For adsorbents with small micropores, the adsorption mechanism is mainly chemical, once a stronger binding of the adsorbate to the adsorbent pore wall occurs. For larger molecules that cannot access to pores, this enhanced adsorption does not occur. As the pores increase in size, adsorption becomes continuously a physical (or multi-layer) process [46]. The morphology of adsorbent/biosorbent after sorbate second leaching was also observed in order to evaluate the effect of those processes on it. Sepiolite (Figure 3B) becomes more fibrous, with a rougher surface, meaning that the exposure to the extraction solvent (aqueous solution with 20% of acetonitrile) may have worn out its surface, becoming more polished. For pine bark (Figure 3D) and cork waste (Figure 3F) differences in morphology were not observed.

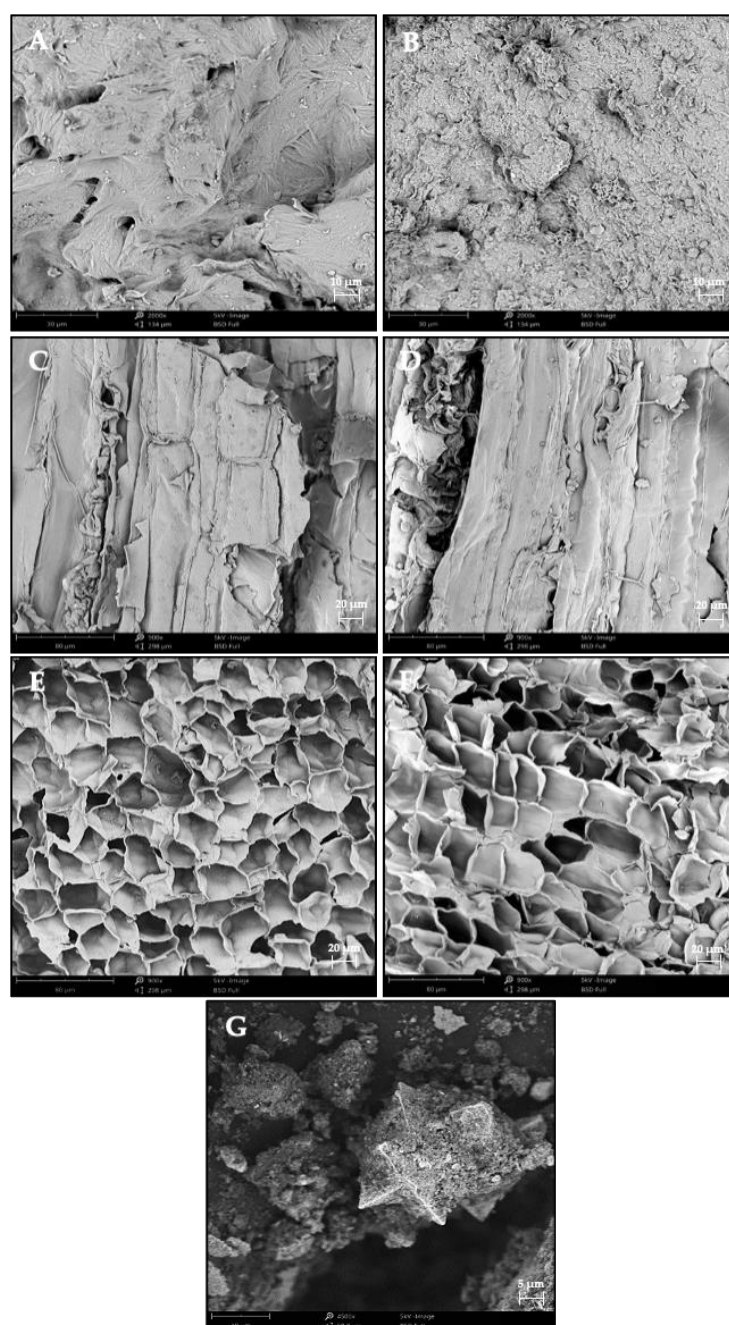


Figure 3. SEM micrographs at various magnifications of raw sepiolite (A), pine bark (C), cork (E), activated rubber char (G) and sepiolite (B), pine bark (D) and cork (F) after two regeneration cycles.

The ATR-FTIR spectra of sepiolite, cork and pine bark in their natural form, as well as after the first and second desorption steps, were recorded in the region of 400–4000 cm^{-1} and are shown in Figures 4–6, respectively. Analyses were performed to evaluate possible changes on surface functional groups after the regeneration process, and therefore to clarify the atrazine adsorption mechanism. In Figure 4, the spectrum of raw sepiolite is shown and the characteristic stretching vibration of -OH groups attached to octahedral Mg^{2+} located in the interior blocks are evidenced, at 3690 cm^{-1} . At 3581 cm^{-1} , the Si-O band is verified. From 3000 to 4000 cm^{-1} , the broad band is due to h-O-H vibrations. In addition, the band at 1658 cm^{-1} is related to the -OH bond and at 1197 cm^{-1} , as well as at 940 cm^{-1} , vibrations can be attributed to the Si-O combination. The 1024 cm^{-1} band corresponds to the Si-O-Si vibrations, and the one at 450 cm^{-1} to the Si-O-Mg link, and, at 653 cm^{-1} , there is the bending vibration of Mg-OH. Sepiolite impurities derived from dolomite are also detected at 1443 cm^{-1} [54,55]. Comparing the bands between the spectra of the raw sepiolite with the ones after exposure to the desorbing solvent, for both leaching steps, no substantial differences were detected (the 1443 cm^{-1} band from dolomite is the one that does not appear). So, it can be considered that the chemical structure of sepiolite is not affected after two regeneration cycles. Natural cork spectra (Figure 5) display several absorption peaks, indicating the complex nature of this biomaterial. The band at 3400 cm^{-1} represents -OH groups, and the bands observed at 2923 cm^{-1} to 2853 cm^{-1} could be assigned to the C-H stretch. The peaks around 1760 cm^{-1} and 1638 cm^{-1} correspond to the C=O stretching. The absorption peak resulting from the C-O bond is observed at 1036 cm^{-1} [56]. The principal constituents of Portuguese *Quercus suber* L. can be identified in these cork spectra as suberin, at 2923, 2853 and 1760 cm^{-1} , guaiacyl-type lignin at 1513, 858, and 816 cm^{-1} , polysaccharides at 1100 and 1036 cm^{-1} and extractives at 1603 and from 1457 to 1300 cm^{-1} [57]. Comparing the bands between the spectra of the cork in its natural form and after two desorption processes, the initial peaks are still observed, meaning that cork material after 2 regeneration cycles remains chemically unalterable, not affected by the desorption processes. As it can be seen in Figure 6, raw *Pinus pinaster* bark spectrum evidences at 3400 cm^{-1} the stretching vibration of the bond between oxygen and hydrogen. The bands at 2920 cm^{-1} and 1450 cm^{-1} can be assigned to the stretching of the C-H bond in the aromatic and aliphatic structures. The bands at 1610 cm^{-1} and 1510 cm^{-1} are attributed to the aromatic C-C skeletal vibrations, and the band around 1733 cm^{-1} results from the stretching vibrations in C-O carbonyl structure. At 1160 cm^{-1} and 1210 cm^{-1} , the stretching of C-O-C in the cellulose and hemicellulose is detected [58,59]. The phenolic -OH and aliphatic -CH stretch vibrations can be identified at 1364 cm^{-1} . Vibrations of -CO and aromatic -CH are detected at 1100 cm^{-1} . The 860, 820 and 773 cm^{-1} bands indicate the -CH bending vibrations from aromatic rings, related to phenolic compounds [60]. In this spectrum, the distinct signal at 1036 cm^{-1} is identified, produced by the aliphatic C-O stretching [58]. When comparing raw pine spectra with the ones obtained after two desorption steps, no substantial differences occur, in contrast to the other materials.

3.2. Adsorption Kinetics Modelling

The assessment of adsorption kinetics can support the definition of the adsorption pathway and probable mechanism involved. Figure 7 shows the experimental data and the fitting kinetics models for the adsorption of atrazine (at 2 mg/L) onto the waste biomaterials/materials. Atrazine concentration measured on a blank test remained unchanged during the experiment. Equilibrium is reached after 56 h for sepiolite, 72 h for cork and 8 days for pine bark, while for the powder-activated rubber char, this stage is attained after 14 h. The percentages of atrazine adsorbed at equilibrium time were approximately 22%, 36% and 50% for sepiolite, cork and pine bark at 5 g/L, respectively, and 100% for activated rubber char at 1 g/L. Results indicate that the adsorption of atrazine is initially fast (due to the availability of adsorption sites), and after a period of time the retention becomes slower, until equilibrium is reached. The most common kinetics models used to explain the sorption processes were used to evaluate the kinetic parameters, such as the PFO and

PSO. For both models, the experimental q_e values are in agreement with the calculated ones. Although both models fit experimental data with high correlation coefficient values (R^2), the PSO model showed the best fit for the generality of the sorbents. Comparing the k_2 value (Table 3) for the studied materials, the adsorption rate of atrazine follows this sequence: sepiolite > cork > rubber char > pine bark. The waste-based materials without pretreatment, sepiolite, cork and pine bark have the capacity to retain atrazine effectively, in their natural form, without resorting to chemical pretreatments.

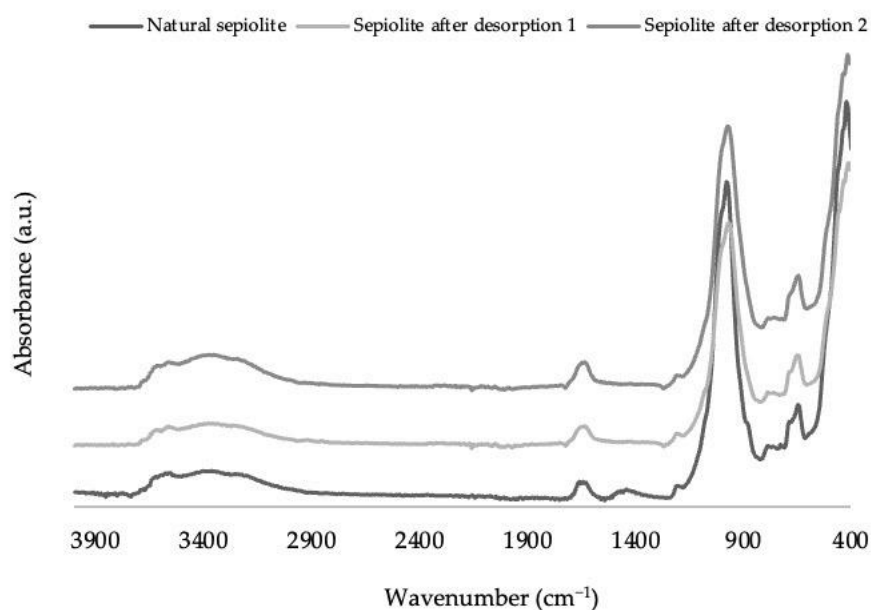


Figure 4. ATR-FTIR spectra of natural sepiolite and after two cycles of adsorption-desorption with a solution with 20% of acetonitrile.

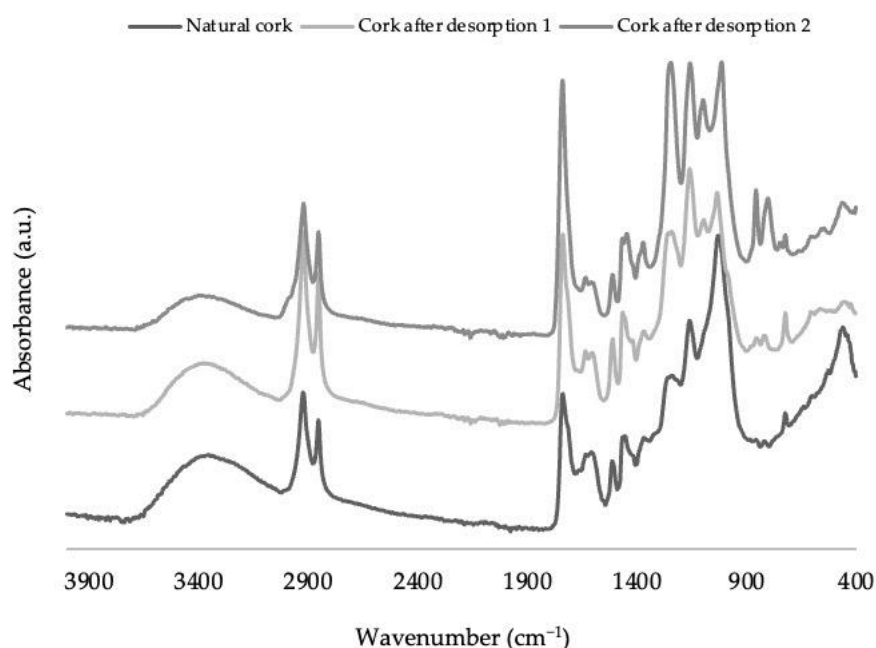


Figure 5. ATR-FTIR spectra of natural cork waste and after two cycles of adsorption-desorption with a solution with 40% of acetonitrile.

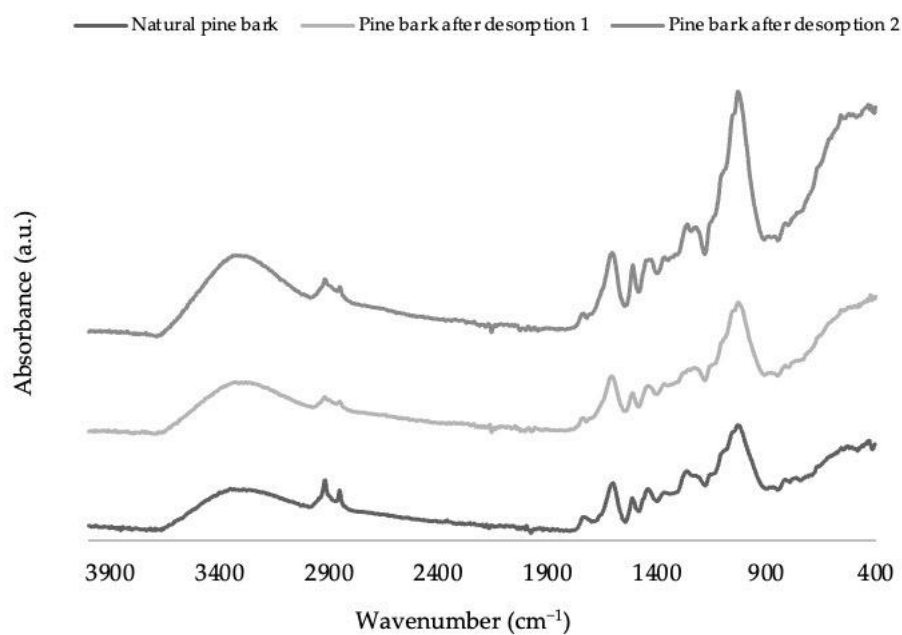


Figure 6. ATR-FTIR spectra of natural pine bark waste and after two cycles of adsorption-desorption with a solution with 40% of acetonitrile.

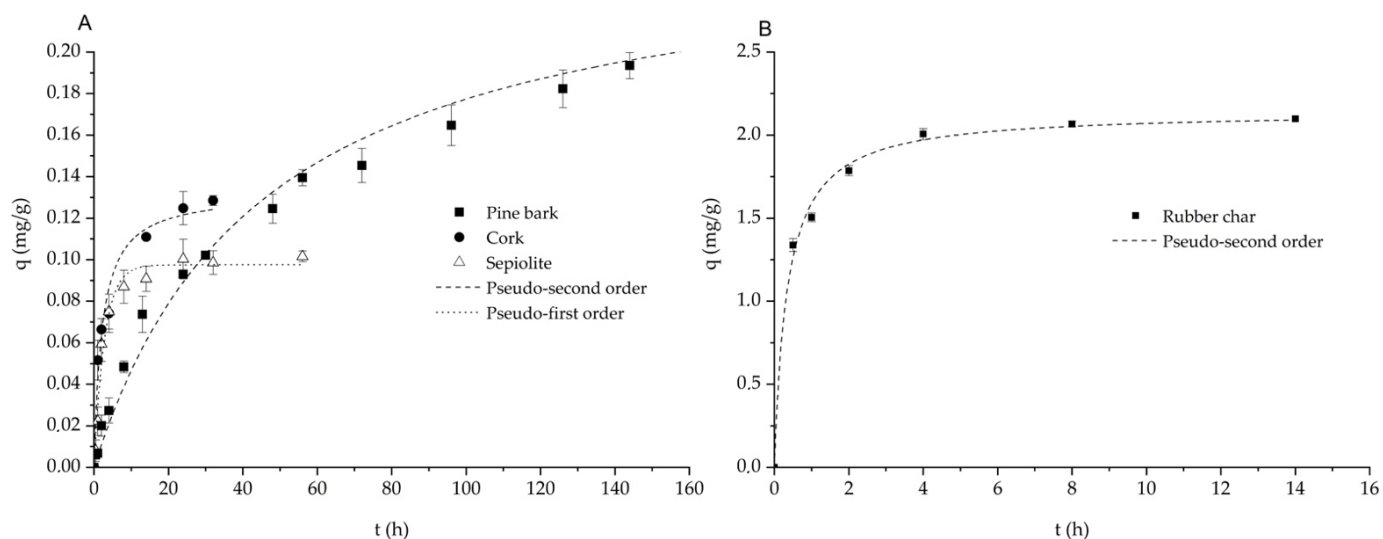


Figure 7. Adsorption of atrazine along time and fittings by the PFO and PSO kinetic models: (A) pine bark, cork and sepiolite; (B) activated rubber char. Experimental conditions: $C_{\text{Atrazine}} = 2 \text{ mg/L}$, biosorbent/adsorbent dose (A) 5 g/L , (B) 1 g/L .

The development of materials with high carbon content, such as the rubber char, with mesoporosity, is important to achieve higher adsorption capacities, as well as faster adsorption kinetics. In addition, the particle size of an adsorbent also plays a significant role in adsorption capacity and rate. This rate tends to increase when particle size decreases, by increasing mesopore volume and S_{BET} [61] and reducing interior diffusional rate limitations. In this study, the rubber char particle has a substantially smaller size than the other materials and is, in fact, the one that achieves an equilibrium stage faster and with a higher uptake value, suggesting that atrazine can be easily adsorbed on the outer surface of the material [62].

Table 3. PFO and PSO model fittings for the adsorption of atrazine onto the different waste materials.

Waste	PFO			PSO		
	q_e	k_1	R^2	q_e	k_2	R^2
Cork	0.351 ± 0.074	0.120 ± 0.007	0.932	0.133 ± 0.006	3.514 ± 0.817	0.973
Pine bark	0.208 ± 0.009	0.021 ± 0.003	0.972	0.257 ± 0.011	0.086 ± 0.014	0.986
Sepiolite	0.098 ± 0.003	0.354 ± 0.043	0.977	0.108 ± 0.005	3.976 ± 0.884	0.970
Rubber char	2.000 ± 0.070	1.760 ± 0.285	0.968	2.143 ± 0.039	1.343 ± 0.167	0.994

q_e —adsorption capacity at equilibrium (mg/g); k_1 —constant of the PFO model (min^{-1}); k_2 —constant of the PSO model (g/(mg.min)); R^2 —coefficient of correlation.

3.3. Adsorption Equilibrium Modelling

Adsorption isotherms are useful for establishing the adsorption capacity of sorbents and for describing their interaction with the adsorbate. In this study, the relation between q_e and C_e was fitted by several different isotherms for water and wastewater treatment, and just the best fitting ones for the selected adsorbents/biosorbents are presented in Table 4, namely Freundlich and three-parameter Langmuir–Freundlich (Sips). The nonlinear regression was used in this analysis to avoid the errors associated with the commonly used linearized models. Figure 8 shows the results obtained from the equilibrium adsorption experiments fitted with the isotherm models. According to Table 4, the Freundlich model is the one that best fits the isothermal adsorption onto cork, sepiolite and activated rubber char, while the Sips model is the one that more adequately fits the isothermal adsorption onto pine bark.

Table 4. Isotherm parameters obtained from the fitting to experimental results on the adsorption of atrazine onto the different waste materials.

Waste	Sips			
	q_{\max}	K_S	R^2	m_S
Pine bark	0.477 ± 0.177	0.567 ± 0.338	0.999	0.64 ± 0.132
Waste	Freundlich			R^2
	K_F	n_F		
Cork	0.209 ± 0.010	0.832 ± 0.062		0.999
Sepiolite	0.128 ± 0.013	1.880 ± 0.246		0.946
Rubber char	8.356 ± 0.548	6.344 ± 1.807		0.924

The Freundlich model is suitable for heterogeneous adsorbent surfaces, and it can be applied to non-ideal or multilayer adsorption by surfaces of varied affinities. n_F and K_F are Freundlich constants which denote the adsorption intensity and capacity, respectively. When $n_F < 1$ the adsorption process is chemical, but if $n_F > 1$, adsorption becomes a favorable physical process [62]. According to Table 4, sepiolite and rubber char present $n_F > 1$, suggesting a physical adsorption process, while cork (with $n_F < 1$) retains atrazine chemically. The highest K_F value was attained for rubber char, demonstrating its higher adsorption capacity. The Sips model results from the combination of Langmuir and Freundlich, and predicts a heterogeneous adsorption system, thereby avoiding the limitations associated with the increased adsorbate concentration. When the concentration of the adsorbate is low, the model reduces to Freundlich isotherm, while for high concentrations, it predicts a monolayer adsorption process on a homogeneous surface (Langmuir model) [63]. The m_S parameter gives information about the degree of surface non-homogeneity. heterogeneous adsorbents present m_S values close to 0, while m_S values closer to 1 indicate a material with relatively homogeneous binding sites [64]. Pine bark presents an m_S value closer to 1, suggesting that its binding sites have the same adsorption affinity, homogeneously distributed over its surface. In terms of maximum adsorption capacities, q_{\max} ,

activated rubber char, is the one that presents the highest value, followed by cork, sepiolite and pine bark, sequentially. Rubber char is the adsorbent with the highest atrazine adsorption capacity since it has enhanced physical properties, as described in the previous section (higher surface area and micropore volume). It is reported that adsorbents/biosorbents without any kind of physical or chemical treatment normally present lower adsorption capacities when compared with the commercial/synthetic ones [15]. Among the tested biomaterials/materials without pretreatment, cork was the one that showed the best performance in terms of atrazine retention; 0.456 ± 0.034 mg/g. Adsorption of atrazine on cork has a strong concurrency with adsorption of water on this biomaterial. On cork, water is firstly adsorbed on hydrophilic sites constituted by hydroxyl and methoxyl groups and then water adsorption continues by clusters formation around the hydrophilic sites. Water adsorption isotherms in cork present the same profile as atrazine [65,66]. Statistical analysis shows no significant differences between biowaste/waste performance. When comparing the adsorption capacity of biowaste/waste (without pretreatment) with activated rubber char, a significant difference was found ($p < 0.0001$). The adsorption capacity of these waste materials can be improved through surface modification treatments, which results in a higher affinity for the target pollutant. The methods used to modify the materials can include physical, chemical and biological methods.

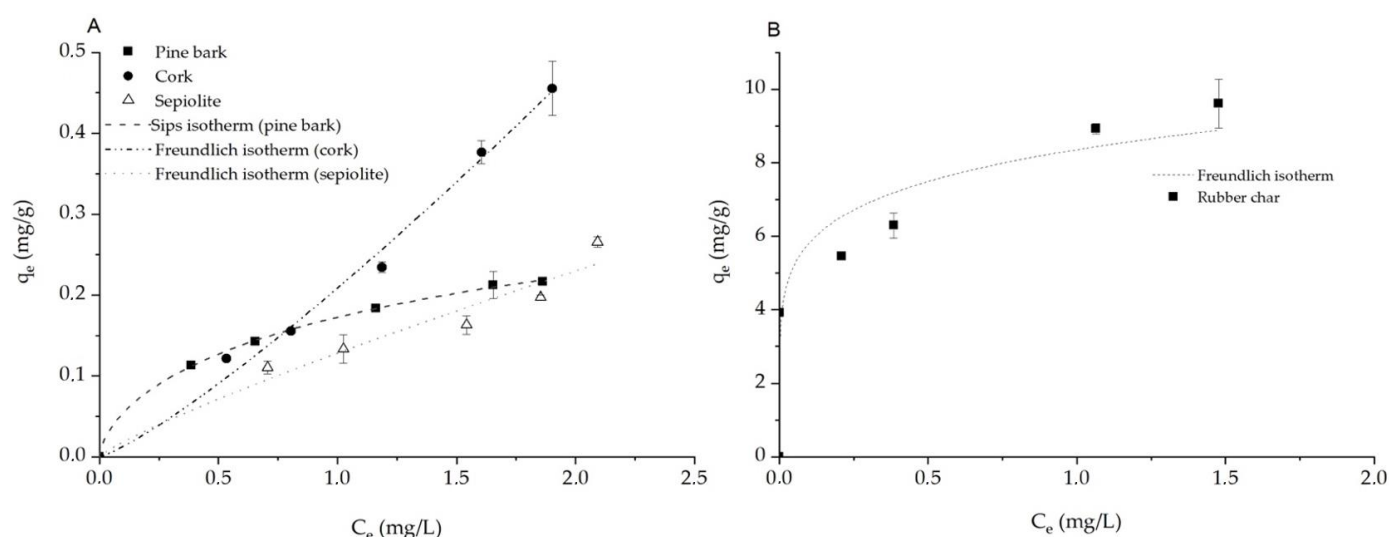


Figure 8. Adsorption of atrazine together with the fittings by the Freundlich and Sips models: (A) pine, cork and sepiolite; (B) activated rubber char. Experimental conditions: $C_{\text{Atrazine}} = 2$ mg/L, biosorbent/adsorbent dose in the range (A) 1–15 g/L and (B) 0.05–0.75 g/L.

3.4. Desorption Evaluation

The selection of a suitable desorption eluent, with a high affinity for the sorbate and able to remove it from the surface of the sorbent, without substantially changing its morphology and efficiency, while being competitive and environmentally friendly, is seen as challenge in the field of biosorption [31].

The desorption of atrazine from sepiolite, cork and pine bark was evaluated, aiming to assess their regeneration/recycling potential. After one adsorption step, each material loaded with atrazine was placed in contact with different leaching agents. The increase in atrazine concentration in the solution was measured over time for 24 h. Figure 9 shows the atrazine desorption efficiency for waste biomaterials/materials using different eluents and different operation conditions (temperature and percentage of acetonitrile in aqueous solution). After 24 h of operation, around 100% of atrazine was recovered from sepiolite using an aqueous solution with 20% of acetonitrile, while for cork and pine bark, recoveries of 94% and 98%, respectively, were attained using an aqueous solution with 40%

of acetonitrile. These results evidence the reversible character of atrazine adsorption onto the materials. An increase in acetonitrile content was needed in the case of cork and pine bark to reach similar desorption values to those attained for sepiolite.

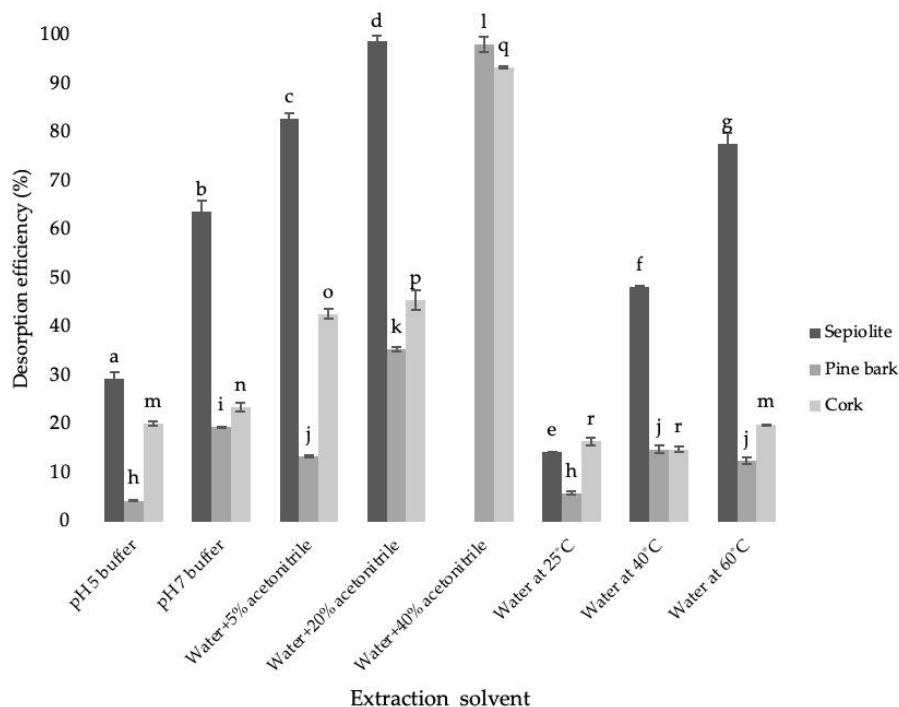


Figure 9. Atrazine desorption efficiency for sepiolite, pine bark and cork, using different solvents and operation conditions, after 24 h of experiment. Different letters show significant differences ($p < 0.05$) between extraction solvents for the same waste biomaterial/material. Sepiolite (a–g), pine bark (h–j) and cork (m–r).

An organic solvent such as acetonitrile increases atrazine solubility in water, justifying its selection for this desorption study. The use of methanol as the most adequate extraction solvent for atrazine desorption from synthetic polymers was demonstrated in a recent study, achieving 73.5% as maximum atrazine desorption percentage [67]. In the same study, it was concluded that higher efficiency values are reached for all materials when using a lower content of organic solvent, which minimizes the environmental impact of this process. Thus, atrazine recovery from these biomaterials/materials can be easily and successfully obtained through extraction with aqueous acetonitrile solutions, which is a rapidly and highly biodegradable solvent.

For sepiolite, a considerably higher desorption efficiency was reached using water at 60 °C, in comparison to the recoveries attained at 25 °C and 40 °C. These results confirm the reversible nature of the exothermic adsorption process. However, this tendency was not as evident for cork and pine bark as for sepiolite.

The desorption efficiency increased for all materials with the increase in the pH of the buffer from 5 to 7. With pH 5 buffer as acidic solvent, atrazine desorption reached 30%, 20% and 5% of the original load from sepiolite, cork and pine bark, respectively. Statistical analysis of desorption data is expressed in Figure 9. In the case of sepiolite, all the extraction solvents used for desorption differ from each other ($p < 0.05$). For pine bark and cork, the aqueous solution with 40% of acetonitrile revealed to be the one with the highest difference compared to the other studied solvents ($p < 0.001$).

3.5. PRB Breakthrough Modelling

Assays with continuous flow in fixed-bed columns were carried out as a simulation of an up-scale PRB to evaluate the dynamic removal of atrazine. The overall performance of

fixed-bed columns and some operational parameters such as breakthrough time, saturation time, adsorption capacity and breakthrough curve shape were evaluated. These parameters can be determined by plotting the experimental results in normalized concentration, C/C_0 over time, t . Figure 10 shows the breakthrough curve obtained with the column set-up experiments with a fixed mass of 20 g of cork, pine bark or sepiolite, when exposed to a continuous flow of a solution with 2 mg/L of atrazine.

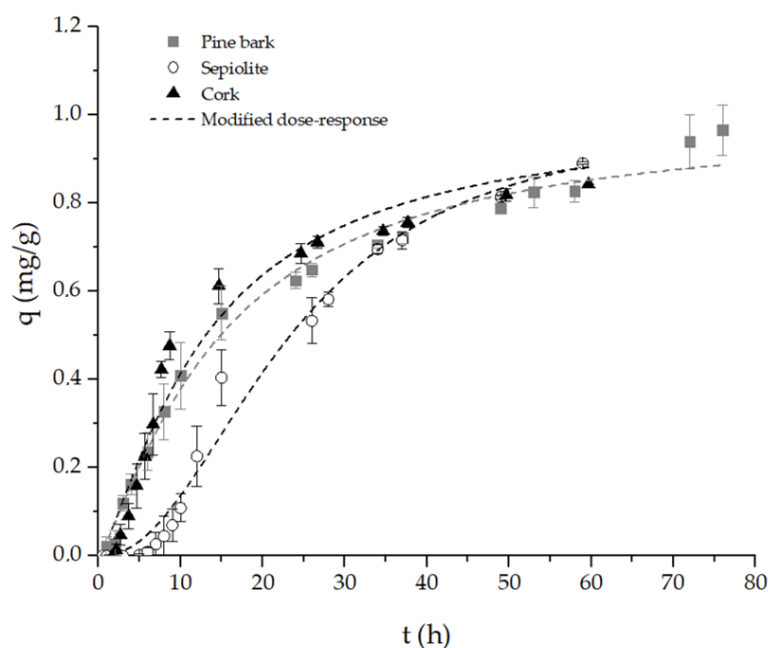


Figure 10. Breakthrough curves of pine bark, sepiolite and cork in fixed-bed columns (flow rate = 1 mL/min).

Mathematical modelling allows the up-scale design and optimized operation, avoiding unnecessary investments and high operational costs by eventual underutilization or oversaturation of beds. Yoon-Nelson and a modified dose-response model were applied to describe the fixed-bed column behavior and the fitting results are shown in Table 5. The modified dose-response was the model that best fitted experimental data ($R^2 > 0.96$ for all the materials), represented in Figure 10, suggesting its suitability to be used for the scale-up purpose. The bed adsorption capacity, q_0 , is a critical indicator of its performance and may be calculated from the breakthrough curve. According to the modified dose-response model, the highest adsorption capacity was attained for sepiolite (23.3 ± 0.8 mg/g), followed by pine bark (14.8 ± 0.6 mg/g) and cork (13.0 ± 0.9 mg/g). Using the Yoon-Nelson model, it was possible to predict the time required to retain 50% of the initial atrazine concentration (τ). Sepiolite achieved the highest value of τ , followed by pine bark and cork, which is in agreement with the adsorption capacity performance predicted by the modified dose-response model. Sepiolite showed the best adsorption performance and, since it is the densest material, a smaller bed length is occupied, which becomes an advantage in terms of experimental operation. Continuous treatments become more feasible than batch processes, allowing an intra-particle diffusion of a bigger amount of atrazine molecules into the pores of the materials. Although batch processes are often used in adsorption studies, the collected data from those experiments are not necessarily applicable to a continuous adsorptive system. Continuous adsorption studies with PRB columns, at lab and pilot scale, are still needed to give real information for a trustworthy scale up.

Table 5. Breakthrough parameters obtained from the fitting models for each biosorbent/adsorbent.

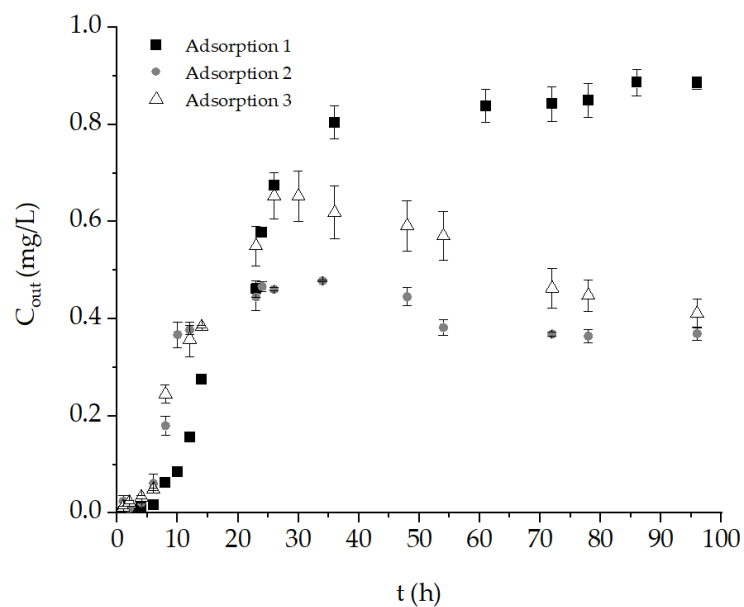
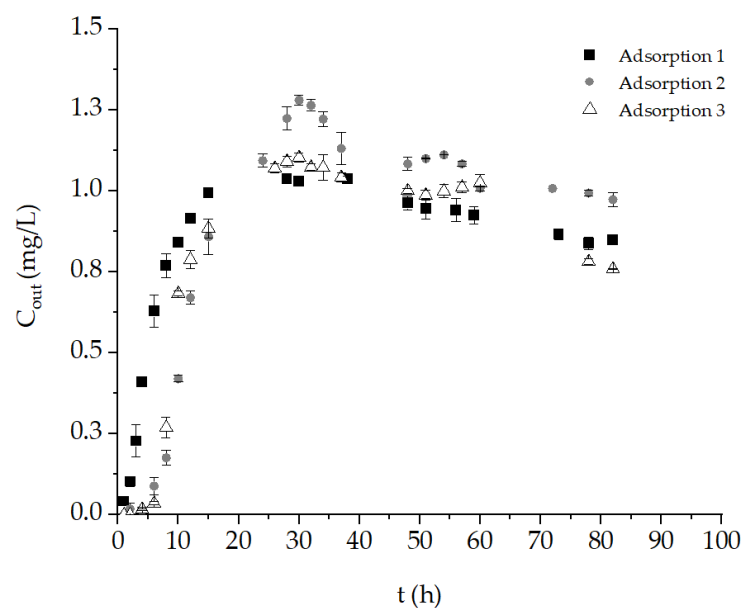
	Yoon-Nelson			Modified Dose-Response		
	$K_{YN} (h^{-1})$	$\tau (h)$	R^2	α	$q_0 (mg/g)$	R^2
Pine bark	0.078 ± 0.011	21.6 ± 2.0	0.902	1.26 ± 0.06	14.8 ± 0.6	0.989
Cork	0.093 ± 0.018	18.2 ± 2.3	0.816	1.32 ± 0.11	13.0 ± 0.9	0.961
Sepiolite	0.118 ± 0.013	26.5 ± 1.3	0.940	2.17 ± 0.13	23.3 ± 0.8	0.984

3.6. Atrazine Retention and Regeneration/Recycling

After the selection of the best desorbing eluent, it is essential to evaluate the number of cycles of adsorption/regeneration that selected materials can cope with, as they may reduce the overall operational costs. These processes can be performed either in batch or continuous procedures; however, when the pollutant retention is conducted in PRB columns, it is better to perform the regeneration step in continuous mode [31]. When the PRB column becomes saturated, the adsorption process is stopped and switched to the desorption/regeneration step. In order to assess the recycling potential of sepiolite, pine bark and cork, successive cycles of adsorption and desorption were performed. Experiments were conducted in columns with the materials placed as PRB. Based on the results of Section 2.4, aqueous solutions with 20% acetonitrile (for sepiolite) and 40% acetonitrile (for pine bark and cork) were used for sorbent regeneration. The assays were initiated by 1 step of adsorption from 2 mg/L of atrazine solution in close-loop (until equilibrium was reached for each material), and then followed by one desorption step in continuous mode over 48 h. The equilibrium of the adsorption process using sepiolite as PRB was reached in 96 h, with pine in 82 h and with cork in 48 h. Three adsorption and two desorption steps were performed, and the values of atrazine removal (%) and respective standard deviations for each step and each material are presented in Table 6. The percentage of atrazine removal after the adsorption processes is calculated based on the difference between the influent atrazine concentration and its outflow concentration, at equilibrium stage. Additionally, atrazine desorption is calculated based on the concentration of atrazine that was retained in the PRB column on each process and its concentration in the desorbing eluent at the end of 48 h of desorption. Figures 11–13 show the output concentration (C_{out}) profile of atrazine over time during adsorption using sepiolite, pine bark and cork in PRB, respectively. Figures 14–16 exhibit the concentration profile of atrazine during desorption on the outflow of the PRB of sepiolite, pine bark and cork, respectively. The results presented on Table 6 show that desorption was performed effectively after the two cycles for sepiolite and pine bark, with performance percentages varying from 85% to 96%. Cork achieved 73% and 55% of desorption capacity after the first and the second process, respectively. The results clearly show that the use of the selected desorption solvents, as well as promoting an effective extraction of the retained pollutant, also promote, in a general way, an improvement of the adsorption capacity during the second adsorption step. After two regeneration cycles, removal percentages increased 30% for sepiolite, 15% for pine bark and remained practically unchanged for cork. This can be explained by the incomplete desorption of atrazine from cork after 48 h, with some adsorption sites remaining unavailable for the second adsorption step. Sepiolite presented the best performance in terms of desorption efficiency, as well as good adsorption stability after regeneration, with the advantage of a smaller environmental impact of the selected elution solvent.

Table 6. Atrazine removal for three sorbents after the adsorption and desorption cycles.

Process	Sepiolite	Pine	Cork
	Atrazine Removal (%)	Atrazine Removal (%)	Atrazine Removal (%)
1st adsorption	51.8 ± 0.7	62.5 ± 1.1	55.7 ± 2.6
1st desorption	84.8 ± 2.9	95.5 ± 0.6	72.9 ± 1.0
2nd adsorption	82.6 ± 2.2	67.9 ± 1.3	56.4 ± 2.0
2nd desorption	96.1 ± 0.9	96.2 ± 0.3	55.3 ± 2.7
3rd adsorption	81.3 ± 1.2	77.8 ± 0.1	54.38 ± 0.3

**Figure 11.** Concentration profiles of the outflow during three consecutive atrazine adsorption steps over time, using sepiolite as PRB.**Figure 12.** Concentration profiles of the outflow during three consecutive atrazine adsorption steps over time, using pine bark as PRB.

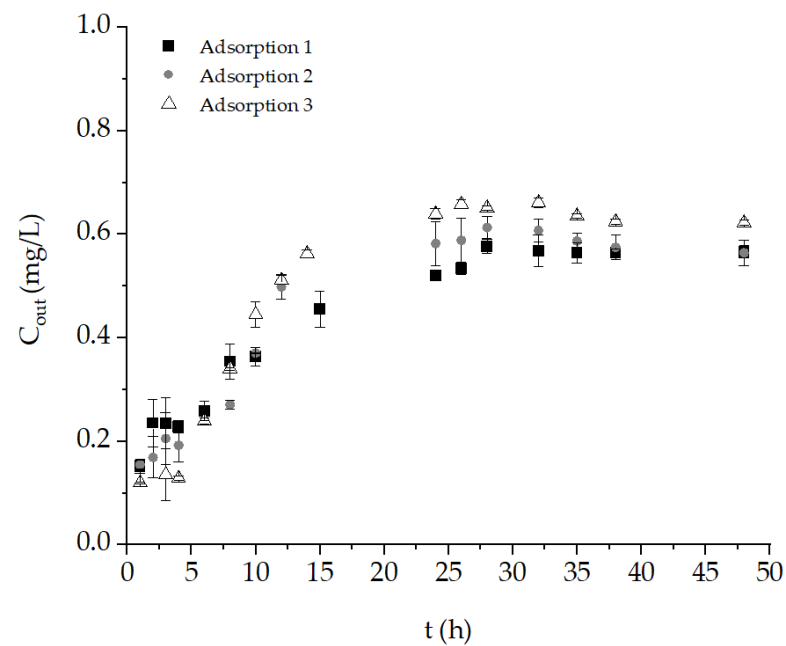


Figure 13. Concentration profiles of the outflow during three consecutive atrazine adsorption steps over time, using cork as PRB.

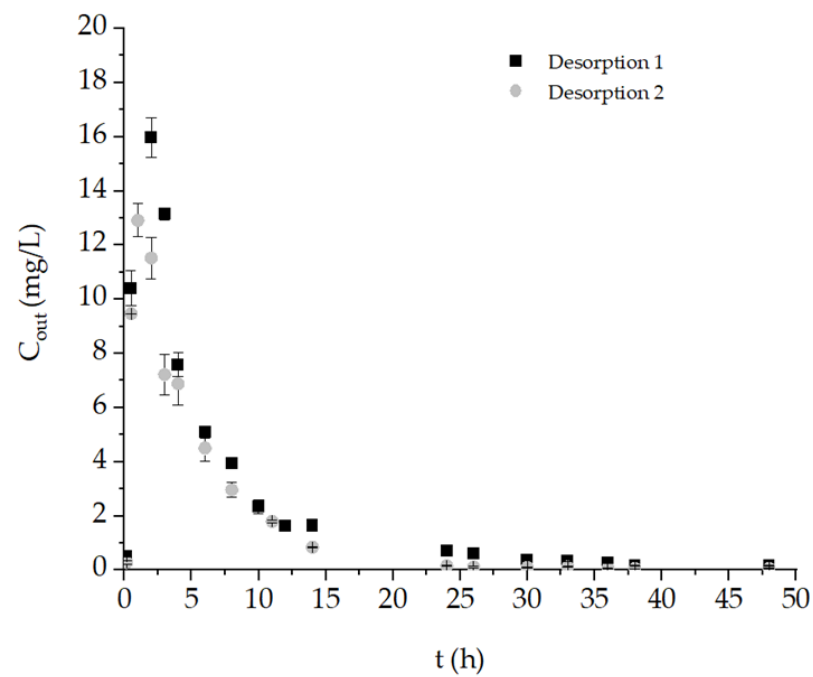


Figure 14. Concentration profiles of the outflow during two consecutive atrazine desorption steps over time, using sepiolite as PBR and 20% of acetonitrile as extraction solvent.

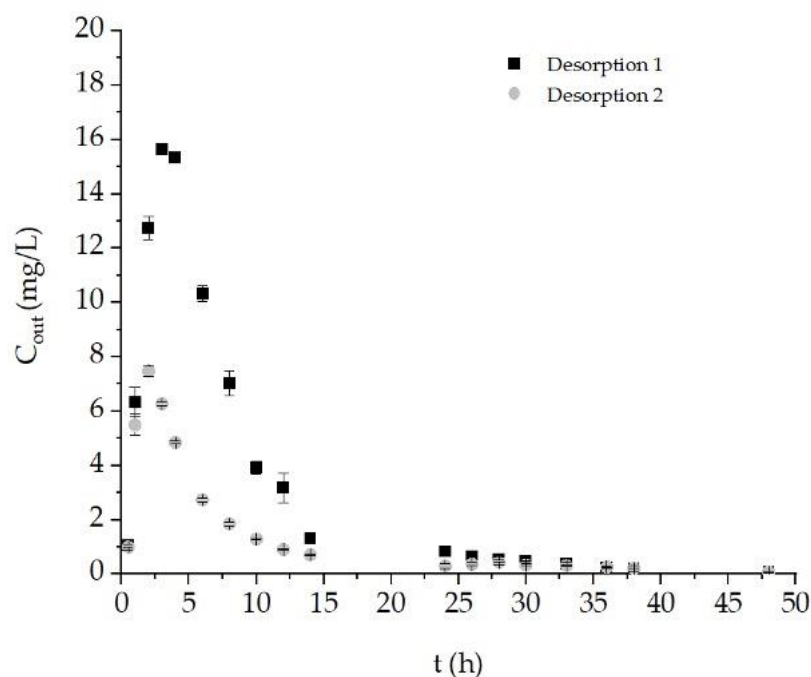


Figure 15. Concentration profiles of the outflow during two consecutive atrazine desorption steps over time, using pine bark as PBR and 40% of acetonitrile as extraction solvent.

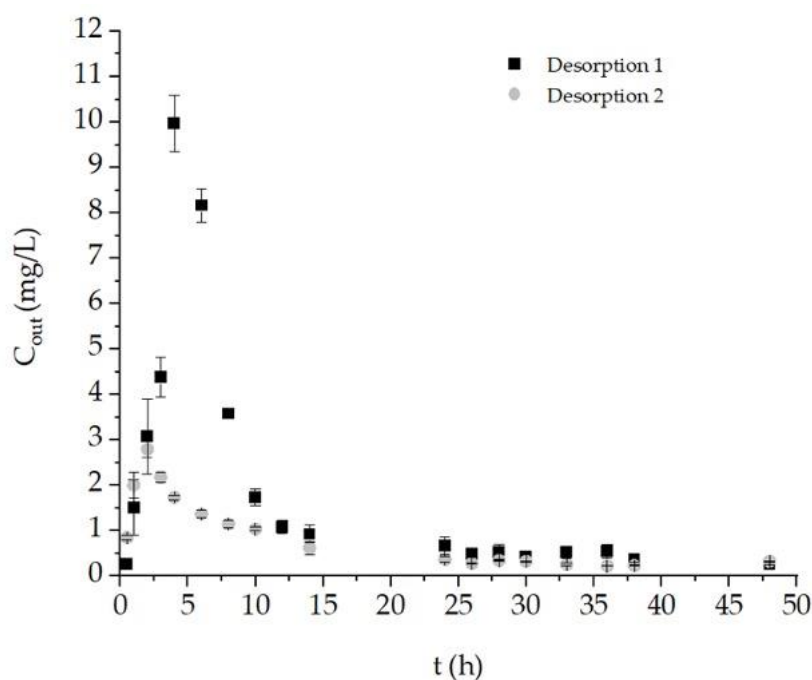


Figure 16. Concentration profiles of the outflow during two consecutive atrazine desorption steps over time, using cork as PBR and 40% of acetonitrile as extraction solvent.

Previous studies have demonstrated the performance of different solvents on the regeneration of adsorbent materials. Mashile et al. [68] demonstrated the efficient use of methanol (up to 95%) to desorb methylparaben and propylparaben and to regenerate waste tire activated carbon-chitosan composite without affecting adsorption capacity. garcía et al. [69] selected pure acetonitrile as an organic desorption agent to regenerate spent biochar, almost achieving a complete desorption of the pollutants, 96.8% and 98.0%, for methyl paraben

and sulfamethoxazole, respectively. In the present study, high desorption capacities are also reached, but lower environmental impact solvents are used while maintaining the adsorption capacity of the materials. On this basis, it is possible to conclude that sepiolite, cork and pine bark can be regenerated and reused at least three times, without any loss in their adsorption efficiency, while acquiring an added value and favoring circular economy.

4. Sustainability Assessment and Lifecycle Perspective

It is common knowledge that AC is the most adopted adsorbent in the field of wastewater treatment, since it has the capability to efficiently retain a wide range of pollutants. However, its widespread use often becomes disadvantageous due to its high production cost (unaffordable to underdeveloped countries), difficult regeneration and end-of-life disposal options [70]. Additionally, the use of AC induces high environmental impacts such as ecotoxicity, acidification, ozone depletion and fossil fuel depletion [71]. Biosorbents have been recognized as an environmentally sustainable solution for wastewater treatment. In addition to their capacity to retain different pollutants, and the fact that they are available on a sustainable basis, their low cost, biodegradability and reduced toxicity character are important advantages to consider. The use of waste-based biomaterials/materials contributes to environmental sustainable growth, since it reduces waste, as well as promotes the recovery and reuse of materials [15]. The reuse of residues allows their life cycle to increase and energy requirements to decrease, resources and emissions [72]. Moreover, it allows the waste disposal problem and the costs for producing new adsorbents for water treatment to be reduced [31]. Through waste valorization, a circular and sustainable economy is promoted, a prevailing priority in the EU in order to achieve a continuous decrease in the negative environmental effects of services and products throughout their life cycle [73]. Bioeconomy is meant to reduce the dependency on natural resources by converting biomass and organic waste into diversified end-products and materials, and providing competitive goods in an environmentally friendly way [74]. This study is focused on the recycling of biological and natural resources waste, which is in line with the expected environmental policies. The sorbent materials, sepiolite, cork and pine bark were tested without any previous chemical treatment, with reduced waste generation (only the one produced by milling and washing steps) so they are good choices to be used as sorbents. As well as being non-toxic materials, they are selective towards the target pollutant, are easy to operate in PRB due to their particle size and are regenerable and reusable. Exhausted sorbents can be also regenerated by successive adsorption/desorption cycles using acetonitrile aqueous solutions, which allows the further transference of atrazine into new solutions, for possible reuse. An economic and environmental evaluation should be taken in consideration to select the material to perform an adsorption process.

5. Conclusions

This study shows the adsorption potential of waste-based biomaterials/materials without resorting to chemicals for the removal of atrazine from water.

Process kinetics were satisfactorily described by the PSO model for sepiolite, cork and pine bark. The Freundlich model fits the adsorption isotherms for cork and sepiolite, while the Sips model fits adsorption on pine bark more adequately. Kinetics and equilibrium of atrazine adsorption onto activated rubber char from waste rubber were also evaluated as a comparative term for the other materials without treatment.

Atrazine desorption feasibility was evaluated in batch systems with different extraction solvents. In 24 h, 100% of atrazine was recovered from sepiolite using an aqueous solution of 20% acetonitrile, while from cork and pine bark the highest values of 98% and 94% were reached, respectively, using solutions of 40% acetonitrile. These desorbing agents were selected to regenerate sorbents in column recyclability assays.

Continuous adsorption of 2 mg/L of atrazine using sepiolite, cork and pine bark as PRB was performed in columns at lab scale. Breakthrough curves were best fitted by the modified dose-response model for all the tested materials ($R^2 > 0.96$), indicating

its suitability for process design and upscaling. The maximum adsorption capacity for sepiolite was 23.3 (± 0.8) mg/g, 14.8 (± 0.6) mg/g for pine bark and 13.0 (± 0.9) mg/g for cork, and these values were determined by mathematical modelling. Sepiolite was revealed to be the best material in terms of adsorption capacity, with the longest breakthrough time of 11 h, followed by 5 h for cork and 4 h for pine bark.

The recycling potential of sorbents in PRB was assessed by consecutive cycles of atrazine adsorption-desorption in column assays. After two regeneration cycles, the best performance in terms of atrazine recovery was measured for sepiolite with 81%, followed by pine bark and cork with values of 78% and 54%, respectively. The desorption efficiency obtained in the second step of 48 h, reached 96% for sepiolite and pine bark, and 55% for cork. Results show that sepiolite is the best material in terms of atrazine adsorption capacity and stability after regeneration, with high potential for reuse and depending on a leaching agent with smaller environmental impact. The characteristics of the selected sorbents, before and after two cycles of sorption/regeneration, were evaluated by SEM and FTIR analyses and no substantial differences were found in structure or morphology.

Adsorption technology employing waste-based materials/biomaterials can be a sustainable option for wastewater treatment, once it promotes waste valorization, pollution mitigation and environmental protection by reducing natural resources dependency. Through waste valorization, a circular and sustainable bioeconomy is promoted by the increased waste life cycle, a prevailing priority in the EU.

The application of sorbents able to compete with commercial ones is still seen as an emerging research challenge. The present study is in line with the growing concern on herbicide removal, and uses reusable waste with recovery capacity and recycling ability, expected by environmental policies.

Author Contributions: A.L.: Conceptualization, methodology, investigation, writing—original draft; B.S.: supervision, software, writing—review and editing; T.T.: supervision, project administration, funding acquisition, writing—review and editing. All authors have read and agreed to the published version of the manuscript.

Funding: This research was funded by the Portuguese Foundation for Science and Technology (FCT).

Institutional Review Board Statement: Not applicable.

Informed Consent Statement: Not applicable.

Data Availability Statement: The data presented in this study are available on request from the corresponding author.

Acknowledgments: This study was supported by the Portuguese Foundation for Science and Technology (FCT) under the scope of the research project PTDC/AAG-TEC/5269/2014, the strategic funding of UID/BIO/04469/2020 unit and BioTecNorte operation (NORTE-01-0145-FEDER-000004) funded by the European Regional Development Fund under the scope of Norte2020—Programa Operacional Regional do Norte, Portugal. A. Lago thanks FCT for the concession of her PhD grant (SFRH/BD/132271/2017). The authors gratefully acknowledge Tolsa S.A. and Corticeira Amorim, SGPS, S.A. companies for providing sepiolite and cork stoppers materials. The authors also thank Ljiljana Matovic from Department of Materials, Vinča Institute of Nuclear Sciences for her help in the activated rubber char production.

Conflicts of Interest: The authors declare no conflict of interest.

References

1. Birch, G.F.; Drage, D.S.; Thompson, K.; Eaglesham, G.; Mueller, J.F. Emerging contaminants (pharmaceuticals, personal care products, a food additive and pesticides) in waters of Sydney estuary, Australia. *Mar. Pollut. Bull.* **2015**, *97*, 56–66. [[CrossRef](#)]
2. Hakeem, K.R.; Akhtar, M.S.; Abdullah, S.N.A. *Plant, Soil and Microbes: Volume 1: Implications in Crop Science*; Springer: Berlin/Heidelberg, Germany, 2016; pp. 1–366. [[CrossRef](#)]
3. Yue, L.; Ge, C.; Feng, D.; Yu, H.; Deng, H.; Fu, B. Adsorption-desorption behavior of atrazine on agricultural soils in China. *J. Environ. Sci.* **2017**, *57*, 180–189. [[CrossRef](#)] [[PubMed](#)]
4. Chevrier, C.; Cordier, S. Atrazine in municipal drinking water and risk of low birth. *Occup. Environ. Med.* **2005**, *400*–405. [[CrossRef](#)]

5. Almeida Azevedo, D.; Lacorte, S.; Vinhas, T.; Viana, P.; Barceló, D. Monitoring of priority pesticides and other organic pollutants in river water from Portugal by gas chromatography–mass spectrometry and liquid chromatography–atmospheric pressure chemical ionization mass spectrometry. *J. Chromatogr. A* **2000**, *879*, 13–26. [CrossRef]
6. Albanis, T.A.; Danis, T.G.; Hela, D.G. Transportation of pesticides in estuaries of Louros and Arachthos rivers (Amvrakikos gulf, N. W. greece). *Sci. Total Environ.* **1995**, *171*, 85–93. [CrossRef]
7. Almberg, K.S.; Turyk, M.E.; Jones, R.M.; Rankin, K.; Freels, S.; Stayner, L.T. Atrazine Contamination of Drinking Water and Adverse Birth Outcomes in Community Water Systems with Elevated Atrazine in Ohio, 2006–2008. *Int. J. Environ. Res. Public Health* **2018**, *15*, 1889. [CrossRef]
8. European Parliament and the Council of the European Union. Directive 2013/39/EU of the European Parliament and of the Council of 12 August 2013 amending Directives 2000/60/EC and 2008/105/EC as regards priority substances in the field of water policy. *Off. J. Eur. Union* **2013**, 1–17. Available online: <https://eur-lex.europa.eu/LexUriServ.do?uri=OJ:L:2013:226:0001:0017:EN:PDF> (accessed on 15 June 2021).
9. Petrie, B.; Barden, R.; Kasprzyk-Hordern, B. A review on emerging contaminants in wastewaters and the environment: Current knowledge, understudied areas and recommendations for future monitoring. *Water Res.* **2015**, *72*, 3–27. [CrossRef]
10. Gabriela Cara, I.; Jităreanu, G. Application of Low-Cost Adsorbents for Pesticide Removal. *Bull. Univ. Agric. Sci. Vet. Med. Cluj-Napoca Agric.* **2015**, *72*, 37–44. [CrossRef]
11. Suo, F.; Liu, X.; Li, C.; Yuan, M.; Zhang, B.; Wang, J.; Ma, Y.; Lai, Z.; Ji, M. Mesoporous activated carbon from starch for superior rapid pesticides removal. *Int. J. Biol. Macromol.* **2019**, *121*, 806–813. [CrossRef]
12. Cheng, Z.; Feng, K.; Su, Y.; Ye, J.; Chen, D.; Zhang, S.; Zhang, X.; Dionysiou, D.D. Novel biosorbents synthesized from fungal and bacterial biomass and their applications in the adsorption of volatile organic compounds. *Bioresour. Technol.* **2020**, *300*, 122705. [CrossRef]
13. Ravichandran, P.; Sugumaran, P.; Seshadri, S.; Basta, A.H. Optimizing the route for production of activated carbon from Casuarina equisetifolia fruit waste. *R. Soc. Open Sci.* **2018**, *5*, 171578. [CrossRef]
14. De Aguiar, T.R.; Guimarães Neto, J.O.A.; Şen, U.; Pereira, H. Study of two cork species as natural biosorbents for five selected pesticides in water. *Heliyon* **2019**, *5*, e01189. [CrossRef]
15. Silva, B.; Martins, M.; Rosca, M.; Rocha, V.; Lago, A.; Neves, I.C.; Tavares, T. Waste-based biosorbents as cost-effective alternatives to commercial adsorbents for the retention of fluoxetine from water. *Sep. Purif. Technol.* **2020**, *235*, 116139. [CrossRef]
16. Fabre, E.; Lopes, C.B.; Vale, C.; Pereira, E.; Silva, C.M. Valuation of banana peels as an effective biosorbent for mercury removal under low environmental concentrations. *Sci. Total Environ.* **2020**, *709*, 135883. [CrossRef] [PubMed]
17. Omo-Okoro, P.N.; Daso, A.P.; Okonkwo, J.O. A review of the application of agricultural wastes as precursor materials for the adsorption of per- and polyfluoroalkyl substances: A focus on current approaches and methodologies. *Environ. Technol. Innov.* **2018**, *9*, 100–114. [CrossRef]
18. Cao, X.; Ma, L.; Gao, B.; Harris, W. Dairy-Manure Derived Biochar Effectively Sorbs Lead and Atrazine. *Environ. Sci. Technol.* **2009**, *43*, 3285–3291. [CrossRef]
19. Gupta, V.K.; Gupta, B.; Rastogi, A.; Agarwal, S.; Nayak, A. Pesticides removal from waste water by activated carbon prepared from waste rubber tire. *Water Res.* **2011**, *45*, 4047–4055. [CrossRef] [PubMed]
20. Tran, V.S.; Ngo, H.H.; Guo, W.; Zhang, J.; Liang, S.; Ton-That, C.; Zhang, X. Typical low cost biosorbents for adsorptive removal of specific organic pollutants from water. *Bioresour. Technol.* **2015**, *182*, 353–363. [CrossRef]
21. Vischetti, C.; Monaci, E.; Casucci, C.; De Bernardi, A.; Cardinali, A. Adsorption and degradation of three pesticides in a vineyard soil and in an organic biomix. *Environments* **2020**, *7*, 113. [CrossRef]
22. Quintelas, C.; Costa, F.; Tavares, T. Bioremoval of diethylketone by the synergistic combination of microorganisms and clays: Uptake, removal and kinetic studies. *Environ. Sci. Pollut. Res.* **2012**, *20*, 1374–1383. [CrossRef]
23. Vinati, A.; Mahanty, B.; Behera, S.K. Clay and clay minerals for fluoride removal from water: A state-of-the-art review. *Appl. Clay Sci.* **2015**, *114*, 340–348. [CrossRef]
24. Ngulube, T.; Gumbo, J.R.; Masindi, V.; Maity, A. An update on synthetic dyes adsorption onto clay based minerals: A state-of-art review. *J. Environ. Manag.* **2017**, *191*, 35–57. [CrossRef] [PubMed]
25. Uddin, M.K. A review on the adsorption of heavy metals by clay minerals, with special focus on the past decade. *Chem. Eng. J.* **2017**, *308*, 438–462. [CrossRef]
26. Santos, S.C.R.; Boaventura, R.A.R. Adsorption of cationic and anionic azo dyes on sepiolite clay: Equilibrium and kinetic studies in batch mode. *J. Environ. Chem. Eng.* **2016**, *4*, 1473–1483. [CrossRef]
27. Sturini, M.; Speltini, A.; Maraschi, F.; Profumo, A.; Tarantino, S.; Gualtieri, A.F.; Zema, M. Removal of fluoroquinolone contaminants from environmental waters on sepiolite and its photo-induced regeneration. *Chemosphere* **2016**, *150*, 686–693. [CrossRef] [PubMed]
28. Silva, B.; Rocha, V.; Lago, A.; Costa, F.; Tavares, T. Rehabilitation of a complex industrial wastewater containing heavy metals and organic solvents using low cost permeable bio-barriers—From lab-scale to pilot-scale. *Sep. Purif. Technol.* **2021**, *263*, 118381. [CrossRef]
29. Wu, J.; Wang, Y.; Wu, Z.; Gao, Y.; Li, X. Adsorption properties and mechanism of sepiolite modified by anionic and cationic surfactants on oxytetracycline from aqueous solutions. *Sci. Total Environ.* **2020**, *708*, 134409. [CrossRef]

30. Song, N.; Hursthouse, A.; McLellan, I.; Wang, Z. Treatment of environmental contamination using sepiolite: Current approaches and future potential. *Environ. Geochem. Health* **2020**. [CrossRef] [PubMed]
31. Adewuyi, A. Chemically modified biosorbents and their role in the removal of emerging pharmaceutical waste in the water system. *Water* **2020**, *12*, 1551. [CrossRef]
32. Şen, A.; Pereira, H.; Olivella, M.A.; Villaescusa, I. Heavy metals removal in aqueous environments using bark as a biosorbent. *Int. J. Environ. Sci. Technol.* **2015**, *12*, 391–404. [CrossRef]
33. Babiker, E.; Al-Ghouti, M.A.; Zouari, N.; McKay, G. Removal of boron from water using adsorbents derived from waste tire rubber. *J. Environ. Chem. Eng.* **2019**, *7*, 102948. [CrossRef]
34. Acosta, R.; Nabarlantz, D.; Sánchez-Sánchez, A.; Jagiello, J.; gadonneix, P.; Celzard, A.; Fierro, V. Adsorption of Bisphenol A on KOH-activated tyre pyrolysis char. *J. Environ. Chem. Eng.* **2018**, *6*, 823–833. [CrossRef]
35. Acosta, R.; Fierro, V.; Martinez de Yuso, A.; Nabarlantz, D.; Celzard, A. Tetracycline adsorption onto activated carbons produced by KOH activation of tyre pyrolysis char. *Chemosphere* **2016**, *149*, 168–176. [CrossRef]
36. Silva, B.; Tuuguu, E.; Costa, F.; Rocha, V.; Lago, A.; Tavares, T. Permeable Biosorbent Barrier for Wastewater Remediation. *Environ. Process.* **2017**, *4*, 195–206. [CrossRef]
37. Upadhyay, S.; Sinha, A. Role of microorganisms in permeable reactive bio-barriers (Prbbs) for environmental clean-up: A review. *Glob. Nest J.* **2018**, *20*, 269–280.
38. Kumarasinghe, U.; Kawamoto, K.; Saito, T.; Sakamoto, Y.; Mowjood, M.I.M. Evaluation of applicability of filling materials in permeable reactive barrier (PRB) system to remediate groundwater contaminated with Cd and Pb at open solid waste dump sites. *Process Saf. Environ. Prot.* **2018**, *120*, 118–127. [CrossRef]
39. Naidu, R.; Birke, V. *Permeable Reactive Barrier: Sustainable Groundwater Remediation*; CRC Press: Boca Raton, FL, USA, 2015.
40. Kozyatnyk, I.; Yacout, D.M.M.; Van Caneghem, J.; Jansson, S. Comparative environmental assessment of end-of-life carbonaceous water treatment adsorbents. *Bioresour. Technol.* **2020**, *302*, 122866. [CrossRef]
41. Torres, E. Biosorption: A review of the latest advances. *Processes* **2020**, *8*, 1584. [CrossRef]
42. Mandal, A.; Singh, N.; Nain, L. Agro-waste biosorbents: Effect of physico-chemical properties on atrazine and imidacloprid sorption. *J. Environ. Sci. Health Part B* **2017**, *52*, 671–682. [CrossRef]
43. Alam, J.B.; Dikshit, A.K.; Bandyopadhyay, M. Kinetic Study of Sorption of 2,4-D and Atrazine on Rubber granules. *J. Dispers. Sci. Technol.* **2007**, *28*, 511–517. [CrossRef]
44. PubChem. Available online: <https://pubchem.ncbi.nlm.nih.gov> (accessed on 1 February 2021).
45. Atrazine. In *Handbook of Pollution Prevention and Cleaner Production: Best Practices in the Agrochemical Industry*; Cheremisinoff, N.P.; Rosenfeld, P.E., Eds.; William Andrew Publishing: Oxford, UK, 2011; pp. 215–231, ISBN 978-1-4377-7825-0.
46. Pelekani, C.; Snoeyink, V.L. Competitive adsorption between atrazine and methylene blue on activated carbon: The importance of pore size distribution. *Carbon N. Y.* **2000**, *38*, 1423–1436. [CrossRef]
47. Mansour, M. Abiotic degradation of pesticides and other organic chemicals in aquatic systems. *Pestic. Outlook (UK)* **1996**, *7*, 9–10.
48. Lagergren, S. About the Theory of So-Called Adsorption of Soluble Substances. *K. Sven. Vetensk. Handl.* **1898**, *24*, 1–39.
49. Blanchard, G.; Maunaye, M.; Martin, G. Removal of heavy metals from waters by means of natural zeolites. *Water Res.* **1984**, *18*, 1501–1507. [CrossRef]
50. Freundlich, H.M.F. Over the adsorption in solution. *J. Phys. Chem.* **1906**, *57*, 1100–1107.
51. Sips, R. On the structure of a catalyst surface. *J. Chem. Phys.* **1948**, *16*, 490–495. [CrossRef]
52. Yan, G.; Viraraghavan, T.; Chen, M. A new model for heavy metal removal in a biosorption column. *Adsorpt. Sci. Technol.* **2001**, *19*, 25–43. [CrossRef]
53. Yoon, Y.H.; Nelson, J.H. Application of gas Adsorption Kinetics I. A Theoretical Model for Respirator Cartridge Service Life. *Am. Ind. Hyg. Assoc. J.* **1984**, *45*, 509–516. [CrossRef]
54. Largo, F.; haounati, R.; Akhouairi, S.; Ouachtak, h.; El haouti, R.; El guerdou, A.; hafid, N.; Santos, D.M.F.; Akbal, F.; Kuleyin, A.; et al. Adsorptive removal of both cationic and anionic dyes by using sepiolite clay mineral as adsorbent: Experimental and molecular dynamic simulation studies. *J. Mol. Liq.* **2020**, *318*, 114247. [CrossRef]
55. Ongen, A.; Ozcan, K.; Ozbas, E.; Balkaya, N. Adsorption of Astrazon Blue FGRL onto sepiolite from aqueous solutions. *Desalination Water Treat.* **2012**, *40*, 129–136. [CrossRef]
56. Sfaksi, Z.; Azzouz, N.; Abdelwahab, A. Removal of Cr(VI) from water by cork waste. *Arab. J. Chem.* **2014**, *7*, 37–42. [CrossRef]
57. Lopes, M.H.; Barros, A.S.; Pascoal Neto, C.; Rutledge, D.; Delgadillo, I.; Gil, A.M. Variability of cork from Portuguese Quercus suber studied by solid-state ¹³C-NMR and FTIR spectroscopies. *Biopolymers* **2001**, *62*, 268–277. [CrossRef] [PubMed]
58. Md Salim, R.; Asik, J.; Sarjadi, M.S. Chemical functional groups of extractives, cellulose and lignin extracted from native Leucaena leucocephala bark. *Wood Sci. Technol.* **2021**, *55*, 295–313. [CrossRef]
59. Brás, I.; Lemos, L.; Alves, A.; Pereira, M. Application of pine bark as a sorbent for organic pollutants in effluents. *Manag. Environ. Qual. Int. J.* **2004**, *15*, 491–501. [CrossRef]
60. Ferreira-Santos, P.; Genisheva, Z.; Botelho, C.; Santos, J.; Ramos, C.; Teixeira, J.A.; Rocha, C.M.R. Unravelling the biological potential of pinus pinaster bark extracts. *Antioxidants* **2020**, *9*, 334. [CrossRef]
61. Tsai, W.T.; Lai, C.W.; Hsien, K.J. Effect of particle size of activated clay on the adsorption of paraquat from aqueous solution. *J. Colloid Interface Sci.* **2003**, *263*, 29–34. [CrossRef]

62. Aljeboree, A.M.; Alshirifi, A.N.; Alkaim, A.F. Kinetics and equilibrium study for the adsorption of textile dyes on coconut shell activated carbon. *Arab. J. Chem.* **2017**, *10*, S3381–S3393. [[CrossRef](#)]
63. Al-Ghouti, M.A.; Da'ana, D.A. guidelines for the use and interpretation of adsorption isotherm models: A review. *J. hazard. Mater.* **2020**, *393*, 122383. [[CrossRef](#)]
64. Ghalandari, V.; hashemipour, H.; Bagheri, H. Experimental and modeling investigation of adsorption equilibrium of CH₄, CO₂, and N₂ on activated carbon and prediction of multi-component adsorption equilibrium. *Fluid Phase Equilib.* **2020**, *508*, 112433. [[CrossRef](#)]
65. Rawat, S.P.S.; Khali, D.P. Clustering of water molecules during adsorption of water in wood. *J. Polym. Sci. Part B Polym. Phys.* **1998**, *36*, 665–671. [[CrossRef](#)]
66. Lequin, S.; Chassagne, D.; Karbowiak, T.; Gougeon, R.; Brachais, L.; Bellat, J.P. Adsorption equilibria of water vapor on cork. *J. Agric. Food Chem.* **2010**, *58*, 3438–3445. [[CrossRef](#)]
67. Romita, R.; Rizzi, V.; Semeraro, P.; Gubitosa, J.; Gabaldón, J.A.; Gorbe, M.I.F.; López, V.M.G.; Cosma, P.; Fini, P. Operational parameters affecting the atrazine removal from water by using cyclodextrin based polymers as efficient adsorbents for cleaner technologies. *Environ. Technol. Innov.* **2019**, *16*, 100454. [[CrossRef](#)]
68. Mashile, G.P.; Mpupa, A.; Nqombolo, A.; Dimpe, K.M.; Nomngongo, P.N. Recyclable magnetic waste tyre activated carbon-chitosan composite as an effective adsorbent rapid and simultaneous removal of methylparaben and propylparaben from aqueous solution and wastewater. *J. Water Process Eng.* **2020**, *33*, 101011. [[CrossRef](#)]
69. Acevedo-García, V.; Rosales, E.; Puga, A.; Pazos, M.; Sanromán, M.A. Synthesis and use of efficient adsorbents under the principles of circular economy: Waste valorisation and electroadvanced oxidation process regeneration. *Sep. Purif. Technol.* **2020**, *242*, 116796. [[CrossRef](#)]
70. De Gisi, S.; Lofrano, G.; Grassi, M.; Notarnicola, M. Characteristics and adsorption capacities of low-cost sorbents for wastewater treatment: A review. *Sustain. Mater. Technol.* **2016**, *9*, 10–40. [[CrossRef](#)]
71. Thompson, K.A.; Shimabuku, K.K.; Kearns, J.P.; Knappe, D.R.U.; Summers, R.S.; Cook, S.M. Environmental Comparison of Biochar and Activated Carbon for Tertiary Wastewater Treatment. *Environ. Sci. Technol.* **2016**, *50*, 11253–11262. [[CrossRef](#)]
72. Moreira, M.T.; Noya, I.; Feijoo, g. The prospective use of biochar as adsorption matrix – A review from a lifecycle perspective. *Bioresour. Technol.* **2017**, *246*, 135–141. [[CrossRef](#)] [[PubMed](#)]
73. Fritsche, U.; Brunori, G.; Chiaramonti, D.; Galanakis, C.M.; Hellweg, S.; Matthews, R.; Panoutsou, C. *Future Transitions for the Bioeconomy towards Sustainable Development and a Climate-Neutral Economy—Knowledge Synthesis Final Report*; Publications Office of the European Union: Luxembourg, 2020; ISBN 978-92-76-21518-9.
74. Stegmann, P.; Londo, M.; Junginger, M. The circular bioeconomy: Its elements and role in European bioeconomy clusters. *Resour. Conserv. Recycl. X* **2020**, *6*, 100029. [[CrossRef](#)]